

MINERALOGY AND GEOCHEMISTRY OF CONTACT METASOMATIC  
IRON DEPOSITS AT JONES CAMP, SOCORRO COUNTY, NEW MEXICO.

---

A Thesis Presented to  
the Faculty of the Graduate School  
New Mexico Institute of Mining and Technology

---

In Partial Fulfillment  
of the Requirements for the Degree  
Master of Science in Economic Geology

---

by  
Alexandrino Cosme Nogueira

July, 1971

## ABSTRACT

The Jones Camp iron deposits, located 72 miles east of Socorro, New Mexico, consist of tabular to lenticular bodies of massive magnetite-hematite within diabase sills and the Yeso Formation adjacent to a diorite dike. Ore bodies in the diabase sills were probably formed by crystal settling. The ore bodies in limestones and gypsum beds of the Yeso Formation are hydrothermal deposits formed by aqueous solutions rising along the margins of the dike. As these fluids traveled through the border facies of the intrusive, they leached iron, titanium, magnesium, and calcium and deposited silica, aluminum, sodium, and potassium. Iron derived by leaching of the border facies, possibly supplemented by iron concentrated in the residual fluids, was deposited in the sedimentary wall rocks as replacement bodies.

Emplacement of the diorite dike occurred at shallow depths of the earth's crust with temperatures between 800-900°C and water pressures between 500-1500 bars; eight weight percent of water was estimated in the diorite magma, and the temperature of the intrusive at the contact with the country rock was approximately 600°C.

Tremolite-actinolite, epidote, garnet, and cordierite

are the main contact silicate minerals and were formed between 475-550°C. The contact metasomatic minerals of the albite-epidote-hornfels facies account for more than 90% of the metamorphic minerals.

Extrapolated experimental data for the magnetite-hematite mineral assemblage indicate a temperature of formation between 450-550°C, under moderately oxidizing conditions; fugacities of O<sub>2</sub> played an important role and were limited between 10<sup>-18</sup> to 10<sup>-15</sup> atmospheres. Fugacities of sulfur species were determined to be: SO<sub>2</sub> probably greater than 10<sup>-4.3</sup> atmospheres, H<sub>2</sub>S equal to 10<sup>-2.7</sup> atmospheres, and S<sub>2</sub> equal to 10<sup>-1.4</sup> atmospheres. Values for the fugacity of H<sub>2</sub> was calculated to be 10<sup>-5.5</sup> atmospheres. The fugacity of CO<sub>2</sub> was determined to be higher than 10<sup>2.37</sup> atmospheres. The CO<sub>2</sub> pressure was initially small but reached higher values due to the formation of the contact minerals and replacement of the calcareous rocks.

Transportation of iron occurred in supercritical aqueous solutions probably of acidic character. The solutions probably transported the iron as chloride complexes, although transport is feasible by other mechanisms. The iron-bearing solutions reached a reactive medium (limestones) and they were neutralized, depositing magnetite, hematite, and minor

amounts of pyrite. As the pH of the solutions rose ( from the carbonate ion uptake of hydrogen ion) with the dissolution of limestone, the stability of the iron oxide minerals increased.

## TABLE OF CONTENTS

|   |     |
|---|-----|
| LIST OF TABLES .....                        | vi  |
| LIST OF FIGURES .....                       | vii |
| LIST OF PLATES .....                        | ix  |
| INTRODUCTION .....                          | 1   |
| Purpose and Scope .....                     | 1   |
| Location and History .....                  | 1   |
| Methods of Investigation .....              | 3   |
| Acknowledgments .....                       | 5   |
| GEOLOGY .....                               | 7   |
| Stratigraphy .....                          | 7   |
| Yeso Formation .....                        | 7   |
| San Andres Formation .....                  | 9   |
| Local and Regional Structure .....          | 11  |
| Mineralogy and Petrology .....              | 13  |
| Igneous Rocks .....                         | 14  |
| Contact Silicate Minerals .....             | 27  |
| Ore Minerals .....                          | 37  |
| GEOCHEMISTRY .....                          | 40  |
| Chemical Analyses of Rocks and Ores .....   | 40  |
| Estimated Conditions of Ore Formation ..... | 47  |
| Confining Pressure .....                    | 47  |

|   |    |
|---|----|
| Temperature of the Diorite Dike .....                             | 49 |
| Temperature of Formation of Contact<br>Metamorphic Minerals ..... | 50 |
| Temperature of Formation of Ore Minerals ...                      | 58 |
| Oxygen Pressure in the Ore-forming Fluid ...                      | 61 |
| Fugacity of Sulfur Species .....                                  | 62 |
| Fugacity of Carbon Dioxide .....                                  | 63 |
| Interpretation of Ore Genesis .....                               | 64 |
| Sources of Iron .....   | 64 |
| Sedimentary Rocks .....   | 64 |
| Diabase Intrusives .....  | 65 |
| Dioritic Dike .....   | 68 |
| Transportation of Iron .....                                      | 73 |
| Magmatic Segregation .....  | 73 |
| Hydrothermal Fluids .....   | 74 |
| Deposition of Iron .....  | 82 |
| Physical Controls .....   | 82 |
| Chemical Controls .....   | 82 |
| SUMMARY AND CONCLUSIONS .....                                     | 84 |
| BIBLIOGRAPHY .....  | 87 |
| APPENDIX .....  | 96 |

LIST OF TABLES

Table

|  |    |
|--|----|
| I) Igneous rocks modal analyses .....                                      | 16 |
| II) Plagioclase composition of the intrusive<br>rocks .....                | 18 |
| III) Chemical analyses of igneous rocks and<br>mineralization bodies ..... | 41 |

## LIST OF FIGURES

### Figure

|   |    |
|---|----|
| 1) Location of Jones Camp iron deposit .....  | 2  |
| 2) Plagioclase composition in diabase sills<br>and diorite dike .....   | 24 |
| 3) Albite-epidote-hornfels facies .....   | 35 |
| 4) Hornblende-hornfels facies .....   | 35 |
| 5) Triangular diagram showing composition<br>of the diorite facies .....  | 42 |
| 6) Chemical changes of major elements across<br>contacts between iron bodies, diabase<br>sills and diorite facies .....                   | 43 |
| 7) Chemical changes of minor elements across<br>contacts between iron bodies, diabase<br>sills and diorite facies .....                   | 44 |
| 8) Diagram of lime-alkalies and magnesium-<br>iron ratios of the diorite facies .....   | 45 |
| 9) Beginning-of-melting curves of olivine<br>tholeiite, granite and diorite .....   | 49 |
| 10) Heating of the country rock adjacent<br>to the intrusive .....  | 51 |
| 11) Possible isobaric equilibrium of<br>tremolite .....   | 53 |
| 12) Temperatures and pressures of contact<br>minerals found at Jones Camp deposit,<br>estimated from published experimental<br>data ..... | 57 |



|  |    |
|--|----|
| 13) Stability field of iron oxides<br>in the Fe-O system .....   | 59 |
| 14) Isothermal diagram at 527°C using<br>fugacities of O <sub>2</sub> and S <sub>2</sub> , in the<br>Fe-O-S system ..... | 59 |

TABLE OF PLATES

Plate

|  |    |
|--|----|
| 1) Mottled border facies of the<br>diorite dike .....  | 21 |
| 2) Photomicrograph of the mottled<br>border facies .....   | 22 |
| 3) Photomicrograph of hydrothermal<br>vein in the mottled border facies .....  | 23 |
| 4) Thin, aplitic dike intruding the<br>outer-intermediate facies of<br>the diorite dike .....  | 26 |
| 5) Pseudo-xenolith of the cream, k-feldspar-<br>quartz-hornblende, porphyritic subfacies<br>in the gray-green, feldspathic, equi-<br>granular subfacies of the central facies<br>of the diorite dike ..... | 28 |
| 6) Panoramic of the west boundary of the<br>area .....   | 29 |
| 7) Photomicrograph showing intergrown<br>of actinolite-tremolite with<br>magnetite and hematite .....  | 30 |
| 8) Photomicrograph showing garnet intergrown<br>with tremolite-actinolite .....  | 31 |
| 9) Photomicrograph showing cordierite and<br>actinolite-tremolite .....  | 32 |
| 10) Close up of iron mineralization in<br>gypsum beds .....  | 38 |
| 11) Rhythmic banding of magnetite-hematite<br>in altered diabase .....   | 67 |

|  |    |
|--|----|
| 12) Iron mineralization in limestone<br>and gypsum beds at the contact<br>with the diorite intrusive .....               | 69 |
| 13) Contact metasomatic bodies of<br>magnetite-hematite emplaced<br>in faulted limestones of the<br>Yeso Formation ..... | 70 |
| 14) Close up of magnetite and hematite<br>replacement in limestones adjacent<br>to a fault plane .....                   | 71 |
| 15) Photomicrograph showing incomplete<br>magnetite-hematite replacement in<br>limestone .....                           | 77 |

## INTRODUCTION

### PURPOSE AND SCOPE

The purposes of this thesis are to determine:

- 1) the origin of the iron mineralization in the Jones Camp area.
- 2) the environment and conditions of ore deposition.
- 3) the genetic relationship between the diabase sills and the diorite dike with the ore mineralization.

### LOCATION AND HISTORY

The Jones Camp iron deposits are located on Chupadera Mesa, 72 miles east of Socorro and 52 miles west of Carrizozo, in sections 13 and 19, T 5 S, R 8 E and sections 13-15, 22-24, T 5 S, R 7 E (fig. 1). Access to the mine is provided by a dirt road parallel to N. M. Highway 380 between Bingham and Carrizozo. The mine is 12 miles northeast of Bingham along this road.

The deposits were discovered in 1902 by P. G. Bell and were named in honor of F. A. Jones. Several studies of a general nature were made during the early 1900's by C. R. Keyes (1904); F. A. Jones (1904); N. W. Emmons (1906); F. C. Schrader (1910); and W. Lindgren, L. C. Granton and C. H.

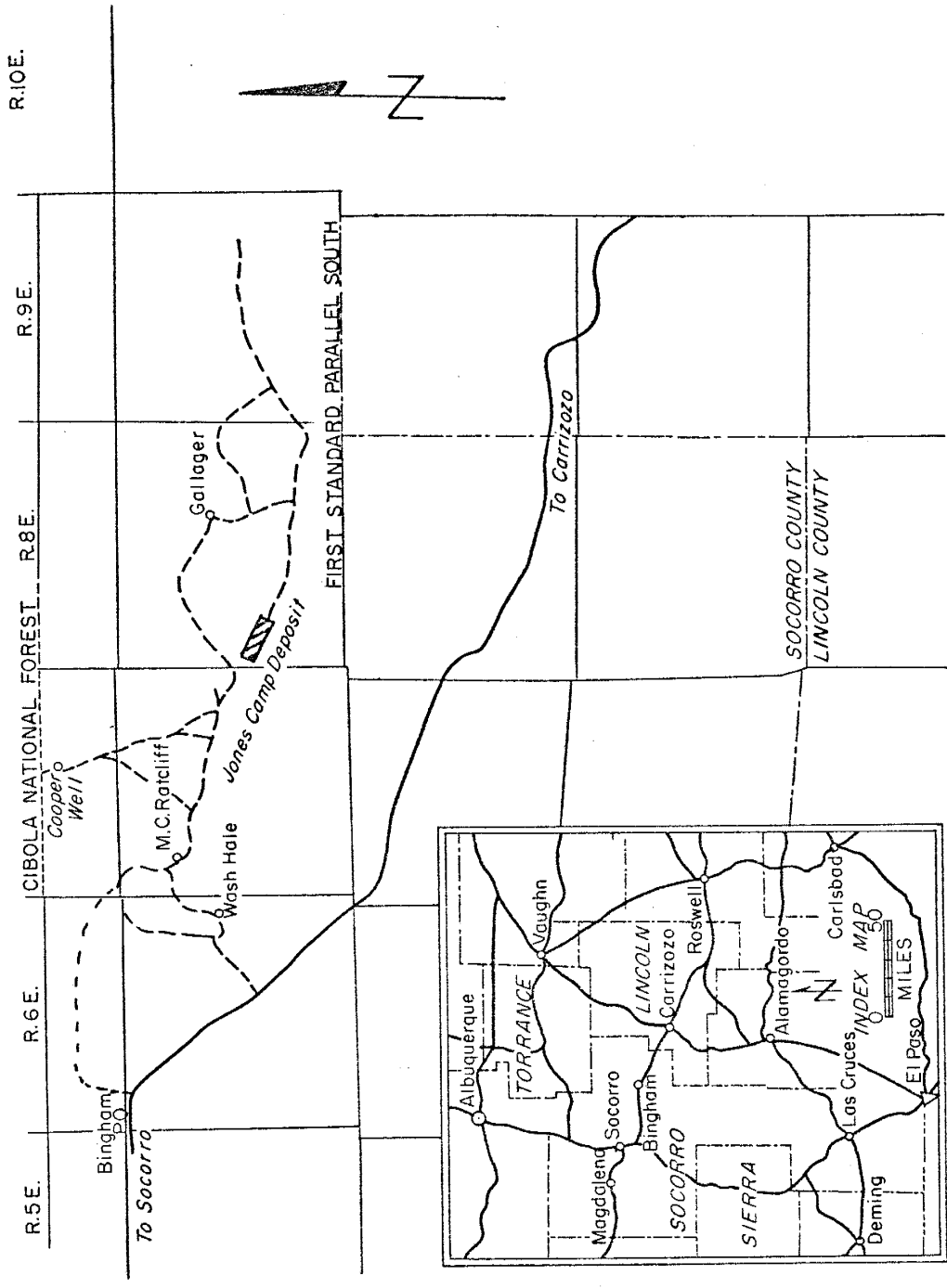


Figure 1

Location of Jones Camp iron deposit, Socorro County,

New Mexico.

0 1 2 3 4 5  
Scale in miles

Gordon (1910). During the Second World War, an extensive exploratory program was suggested by C. H. Johnson in 1942. The exploratory program was carried out by R. M. Grantham of the Bureau of Mines from April to June of 1942. Fifty-eight trenches were excavated and analyses were made of the mineral bodies. At the same time, V. C. Kelley of the U. S. Geological Survey prepared a geological map of the area of greatest mineralization. In 1959, the deposits were core drilled by Cleveland Cliffs Iron Co. The Property presently belongs to the International Mineral Co. and is operated by Carl Dotson of Socorro, N. M.

#### METHODS OF INVESTIGATION

The field work was conducted during the summer of 1969. The U. S. Geological Survey 7½ minute quadrangle map of Broken Back Crater was enlarged to a scale of 1: 2400 (1"=200') from which a mylar topographic base map was prepared.

Petrographic analyses of the principal igneous rocks were performed with the aid of a Swift point counter. Plagioclase determinations were made using three different methods: extinction angles (according to Michel -Levy/ Fouque technique) oil immersion, and x-ray diffraction. The x-ray diffraction technique was used for some minerals when optical determi-

nation was not satisfactory.

Mineralographic studies using optical properties and microchemical tests were performed on polished sections of the ore. Electron-probe analysis of one ore sample was necessary because of the impossibility of using microchemical tests.

The chemical analyses of the principal intrusive rocks were made by x-ray fluorescence using a Norelco 8-position Vacuum Spectrograph. The results were obtained according to the procedures previously described by Leake and others (1969, 1970) and are summarized in Table I. Instrumental parameters used are outlined in Appendix I. The major and minor elements were determined by the ratio of the various elements to the counts collected from a standard rock sample (amphibolite B.L3571; Leake et al, 1969, 1970). This ratio was employed in calibration equations (Appendix II) suggested by Leake to obtain the respective element concentrations. The technique used for sample preparation was:

- 1) Representative rock samples were broken with a steel hammer into small pieces 1-2 cm. in diameter and crushed into smaller fragments in a steel jaw.
- 2) The rock fragments were broken into finer pieces with a hand crusher. The aggregate was then ground in a Tema

agate swing mill until all the powder passed through a 250-mesh nylon sieve.

- 3) Six grams of the homogenized powder was weighed into a plastic vial and one gram of bakelite powder was added.
- 4) After mixing, the powder was placed into stainless steel plattens and compacted with a hydraulic press for three minutes at 25 tons-per-square-inch pressure. The resulting pellet was analysed by x-ray fluorescence.

#### ACKNOWLEDGEMENTS

This thesis was done under the direction of Dr. Charles Chapin to whom the author is indebted for advice and encouragement. Also the author wishes to express his sincere thanks to Drs. Clay Smith and Max Willard members of his advisory committee for their invaluable suggestions. The chemical and electron-probe determinations were provided by Mr. Charles Walker and Mrs. Corale Brierley of the New Mexico Bureau of Mines. The author would also like to thank Drs. Kent Condie and Antonious Budding for their help and cooperation. My classmates Douglas Cowan, Starr Lanphere, James McGlasson and John Sonderegger provided assistance with petrographic studies, microphotographs, x-ray determinations and field relationships.



The author would also like to express his sincere thanks to his wife, Milagros, for her patience and understanding.

## GEOLOGY

### STRATIGRAPHY

The sedimentary sequence which crops out in the study area consists of the Yeso Formation and the San Andres Formation; both are of Permian age (Leonard Series).

#### Yeso Formation:

The Yeso Formation was named by Lee (1909) from a small butte, Mesa del Yeso, 12 miles northeast of Socorro. Needhan and Bates (1943) later described the formation in greater detail. The Yeso Formation has been differentiated into four members by general stratigraphic studies. These members are, in ascending order, the Meseta Blanca, the Torres, the Canas and the Joyita. Only the Joyita member can be easily recognized in the Jones Camp area. Distinction between the Canas and Torres members is extremely difficult because where both are present, the majority of the section belongs to the Canas member and to the upper part of the Torres member. The latter is a dark gray limestone which forms a continuous bench (Bates and others, 1947) parallel to the southern margin of the dike. The Meseta Blanca member is not present in the mapped area although it was observed in a gulch  $1\frac{1}{2}$  miles west of the mapped area at the southern boundary of the main dike.

The Yeso Formation in the Jones Camp area is represented by the upper part of the Torres member, the Canas member, and the Joyita member. The upper part of the Torres member crops out locally in the southern part of the map area. It consists of an initial interval of 12 feet of epidotized gypsiferous sandstones which are friable, medium grained and bluish-gray in color. These are overlain by 9 feet of finely-laminated, gray-to-white gypsum and 8 feet of sericitized and kaolinized rock in a fault zone. The top of the Torres member consists of 8 feet (generally variable) of fetid, gypsiferous, brecciated, black limestone of dolomitic composition (R. Foster, 1971, pers. comm.).

The Canas member is dominated by 200-300 feet of finely-laminated, calcareous and silty gypsum beds which are gray-to-white in color and which contain minor, intercallated sandstones and limestones. The unit contains a basal sandstone which is about 16 feet thick, medium-to-coarse grained, and yellow-to-pink in color. The limestones are gypsiferous, dolomitic, variable in thickness, generally soft and muddy in texture, and gray in color.

The Joyita member consists of about 60 feet of fine-grained, pink sandstones with some siltstone partings and gypsiferous beds toward the top. Its upper contact with the

Glorieta Sandstone is conformable.

### San Andes Formation

The San Andres Formation was originally described by Lee and Girty (1909) from San Andres Mountains, southeast of Socorro. Recent work has subdivided this formation into three members; the Glorieta Sandstone, the Limestone member, and the Upper member. The original description did not include the Glorieta Sandstone. Keyes (1915) first used this name derived from Glorieta Mesa in Santa Fe and San Miguel Counties, New Mexico. Considerable controversy has arisen concerning this member which is considered by many to deserve formational status because of its thickness, regional distribution and distinctive character; however, at present, the Glorieta Sandstone is regarded as a member of the San Andres Formation (U.S. Geological Survey) and will be considered as such in this paper.

The San Andres Formation in the Jones Camp area consists of the Glorieta Sandstone member and the Limestone member. The Glorieta Sandstone forms the base of the San Andres Formation and is composed of 50-100 feet of medium-to-coarse-grained, yellowish-white sandstone. The quartz grains are frequently surrounded by, and stained with, hematite.

The Limestone member comprises the bulk of the San

Andres Formation and is as much as 350 feet thick within the map boundaries. It consists of a thick, resistant sequence of finely crystalline, highly fossiliferous, gray to brownish-gray dolomitic limestone with some interbeds of thin, calcareous, yellow sandstones which are similar to the Glorieta member. Considerable variation in texture exists in the carbonate sequences of this member, with varieties ranging from crystalline limestone to wackestone (Dunham classification).

## LOCAL AND REGIONAL STRUCTURE

The general structure in the area surrounding the Jones Camp deposit is a broad homocline dipping gently eastward. Extensive faulting and numerous north-northwest trending folds disrupt the homoclinal pattern from the Jornada del Muerto basin to Pecos slope. Locally, small domes and flexures are associated with Tertiary intrusives in the Sierra Blanca, Carrizo, Jicarilla, Capitan, and Gallinas mountains. All of these masses except the Capitan intrusive follow a regional north-south trend. The Capitan igneous mass has a west-northwest trend similar to the Jones Camp intrusive indicating a possible relationship between these bodies.

Near Jones Camp the prominent structure is the Chupadera Mesa or platform which has a north-northwest trend and is 45 miles long and varies from 10 to 15 miles in width. The Mesa has a dip of one degree or less in a north easterly direction. It is bounded on the west by the Chupadera anticline. The axis of the anticline passes very close to the western portion of the Jones Camp intrusive. The Chupadera anticline dies out to the south against the homocline of the Oscura block. The eastern boundry of the Chupadera Mesa, is limited by the Chupadera fault (Kelly and Thompson, 1964), that extends from highway 380 north around the eastern nose

of the Jones Camp dike almost to the southern end of Estancia Valley, a distance of nearly 50 miles. Its throw is approximately 350 feet in the central part with the east side down.

The Jones Camp dike is exposed for about 10 miles in west-northwest direction. The general trend of the Jones Camp dike is paralleled by another dike close to the nose of the Chupadera anticline 8 miles north of the deposit and by intrusives at Capitan, Roswell and Acme.

The Jones Camp dike in the area studied strikes north  $70-75^{\circ}$  west, dips steeply south, and has a width of approximately 600 feet. Because of its great length and relatively narrow width together with some indications of faulting along its borders, the author believes that the dike was emplaced along a pre-existing fault. The emplacement was post-Permian and probably of Tertiary age because of its similarity to known Tertiary intrusives in the area. When the dike was intruded, it upturned the strata of the Yeso Formation ( $75^{\circ}$  dips exist close to the dike boundaries) and moderately warped the San Andres Formation into a gentle anticline. This anticline is perpendicular to the regional fold trends (Chupadera anticline, etc.) and seems to have no direct connection with the principal tectonic stresses which caused the folding of the region. The anticline of the Jones Camp area (see gen-

eral cross sections) is believed to be a local effect of dike emplacement.

## MINERALOGY AND PETROLOGY

### General Aspects

The major portion of this investigation involved detailed determinations of the mineralogy, petrology, and chemical composition of the igneous rocks and contact minerals to estimate the origin and conditions of ore deposition. A close spatial relationship is present between the complex diorite dike and the mineralization. Different textural and compositional characteristics were noted in the diorite dike. The nature of these differences needs to be defined. The possibility of multiple dioritic dikes emplaced against different facies of the same intrusive were alternatives that will be discussed later.

The mineralogy of the contact minerals in direct association with the ore minerals and intrusive rocks is relatively simple. Minor quantities of locally occurring meta-silicates, not in equilibrium with the general low grade of metamorphism, were confirmed by x-ray diffraction.



## Igneous Rocks

There is a high degree of textural similarity in the intrusives studied. Textures are holocrystalline to porphyritic with subhedral to anhedral crystals. The average grain sizes of phenocrysts and groundmass are approximately the same; however, feldspar phenocrysts are definitely smaller in the diabase bodies where their maximum size is about 1 mm. The feldspar phenocrysts in the diorite dike reach a maximum size of 5 mm. toward the central facies. The plagioclase typically occurs as elongated laths of subhedral outline and are generally zoned with rims of deuteric alteration. The plagioclases have at least three stages of crystal growth as indicated by mutual interpenetrations. The concentration of orthoclase toward the border of the plagioclases is due to the replacement of the plagioclase edges by more sodic and potassic material.

Graphic intergrowths, microperthitic textures, microcline crystals, and phenocrysts of orthoclase in sutured anhedral grains occur in the most acidic parts of the dike. Needle-like crystals of hornblende are present in almost all the facies, and reaction or alteration textures between amphiboles and pyroxenes occur frequently. Augite, aegerine-augite and sporadic hypersthene constitute the main pyroxenes which are frequently replaced by hornblende. The

hornblende pleochroism varies from moderate to strong with variable colorations of reddish brown, greenish brown, or yellowish green.

Considerable deuteric effects are visible in all facies of the diorite dike. Epidotization is by far the most common alteration; chloritization and sericitization accompanying epidotization have been noticed but are of relatively minor importance. The alteration of plagioclases ranges generally from 20 to 40%. Selective replacement and epidotization of the more calcic cores of plagioclase is distinctive. Magnetite and specular hematite occur as rectangular, euhedral to subhedral crystals, generally associated with ferromagnesian minerals and sphene. Magnetite and sphene replace not only hornblende and pyroxene, but also feldspar. The replacement of feldspar is mainly along twinning planes.

Mineralogical and petrological analyses of the igneous rocks are summarized in table I. They were made by counting between 800 and 1200 points in each thin section. The rocks chosen for the study were selected from approximately 25 thin sections of the igneous intrusives as being as representative as possible.

Plagioclase compositions were determined by a combination of the Michel-Levy and Fouque methods, oil immersion,

Table I

## Igneous Rocks Modal Analyses

| Sample | Qz   | K-spar | Plag. | Hornb | Pyr.  | Magnt.<br>+<br>HmT. | Sphene | Calc. | Apat. | Biot | Epid | Chlor | Descr.     |
|--------|------|--------|-------|-------|-------|---------------------|--------|-------|-------|------|------|-------|------------|
| 30     | 1.08 | 12.67  | 63.37 | x     | 7.00  | 2.27                | 1.84   | 1.41  | x     | -    | A    | A     |            |
| 71     | x    | 9.60   | 73.37 | 6.43  | 2.88  | 3.55                | 1.18   | 2.51  | x     | x    | -    | P     | c.d.f.f.   |
| 72     | x    | 11.54  | 60.61 | 12.33 | 11.14 | 2.30                | 1.30   | x     | x     | -    | A    | A     | o.i.h.f.f. |
| *76    | 5.00 | -      | 60.00 |       | 30.40 | 1-1.50              | 1-1.50 | x     | x     | -    | A    | P     | m.b.f.f.   |
| *77    | 5-10 | -      | 60-65 | -     | 30    | 1.50                | xx     | x     | x     | -    | A    | P     | m.b.f.f.   |
| 83     | -    | 2.41   | 72.53 | -     | 20    | 5.18                | x      | -     | x     | -    | A    | A     | diab.      |
| 156    | 8.30 | 20.40  | 59.43 | 8.63  | xx    | 2.30                | xx     | -     | -     | -    | -    | -     | c.qd.f.f.  |
| 157    | -    | 9.43   | 57.08 | 7.08  | 19.89 | 4.90                | xx     | xx    | x     | x    | -    | -     | i.i.p.f.f. |

x : 0.1-0.5%

xx: 0.5-1%

A : abundant alteration

P : minor alteration

\* : visual estimation

m.b.f. : mottled border facies

o.i.h.f.: outer-intermediate hornblende facies

i.i.p.f.: inner-intermediate pyroxene facies

c.d.f. : central diorite facies

c.qd.f. : central quartz diorite facies

and x-ray diffraction (table II). For the determinations using the Michel-Levy/Fouque method, extinction angles were measured on albite twinning of plagioclases cut perpendicular to the X-axis. The maximum extinction angles were plotted on the low temperature curves of Rogers and Kerr (1959, p. 258) and A. Köhler (1952, p. 101) to obtain the plagioclase composition. Immersion liquids with a calibration interval of 0.002 were used to determine refractive indices; plagioclase compositions were obtained from the refractive indices by using the curves of Rogers and Kerr (1959). The results agreed with determinations made by the Michel-Levy/Fouque method as shown in table II.

The results of x-ray diffraction studies, using the method described by Smith and Yoder (1955), differ significantly with the optical determinations. However, incompatible compositional values were found indicating poor reliability of the x-ray method. Differences in the x-ray parameters can be attributed to potassium content of the plagioclases, as was indicated by Smith and Yoder (1955, p. 635), or to unmixing related to the peristerite solvus (K. C. Condie, 1971, pers. comm.).

The diorite dike is the main intrusive of the area and forms continuous, resistant scarps marked by aligned topog-

Table II

## Plagioclase Composition

| Sample | Michel-Levy-Fouque |               | Refractive indices                                      |                 | X-Ray diffraction distances |                   |
|--------|--------------------|---------------|---|-----------------|-----------------------------|-------------------|
|        | Max. ext. angle    | Comp.         | *Index  | Comp.           | $\Delta_{2\theta}$          | (131) (131) Comp. |
| 71     | 13                 | An-30         | $n_{\alpha} \approx 1.5405$                             | An-25           | 1.50                        | An-20             |
| 72     | 18.5               | An-36         | $n_{\gamma} \approx 1.554$                              | An-36           | 1.90                        | An-59             |
| 73     | 16                 | An-6          | $n_{\beta} \approx 1.536$                               | An-8            | 1.20                        | An-6              |
| 76     | 15<br>21.5         | An-7<br>An-41 | $n_{\beta} \approx 1.536$<br>$n_{\gamma} \approx 1.552$ | An-8.5<br>An-39 |                             |                   |
| 77     | 15<br>22           | An-7<br>An-42 | $n_{\beta} \approx 1.538$<br>$n_{\alpha} \approx 1.548$ | An-11<br>An-39  |                             |                   |
| 78     | 14                 | An-8          | $n_{\gamma} \approx 1.538$                              | An-1, 5         | 1.50                        | An-20             |
| 83     | 26                 | An-47         |   |                 |                             |                   |
| 156    | 20.5               | An-39         | $n_{\beta} \approx 1.550$                               | An-35           | 1.50                        | An-20             |
| 157    | 27                 | An-49         | $n_{\gamma} \approx 1.561$<br>$n_{\beta} \approx 1.556$ | An-48-46        | 1.70                        | An-30             |

\*  $\pm 0,002$

raphic highs. The dike ranges in composition from a diorite in the border and intermediate zones to a quartz-diorite in the central zone. The diabase sills (sample 83) in the vicinity of the diorite dike (samples 71,72,73,76,156,157) have been slightly altered, specially by the addition of elements such as Si and Na.

The composite diorite dike has been divided into the following facies:

- 1) Mottled border facies,
- 2) Outer-intermediate coarse hornblendic facies,
- 3) Inner-intermediate pyroxenic facies, and
- 4) Central facies.

Mottled border facies are situated on both sides of the composite dike and average 100 feet in thickness. They are composed of fine-grained, epidotized, silicified, green to pale green diorite with generally vertical contacts and fine flow banding. The border facies contains intertonguing structures between elliptical or rounded patches of dioritic material, similar to the intermediate hornblendic facies, and finer-grained penetrating tongues of a more epidotized and silicified material, thought to have been altered by ascending hydrothermal solutions. Texturally, this facies is characterized by a fine, felted intergrowth of plagioclase

with minor amounts of orthoclase. Clusters of pyroxene, mainly augite and epidotized pyroxenes and amphiboles, are abundant. These clusters give a pseudo-ophitic texture to the facies which accounts for the mottled character of the rock. Plate 1, and 2.

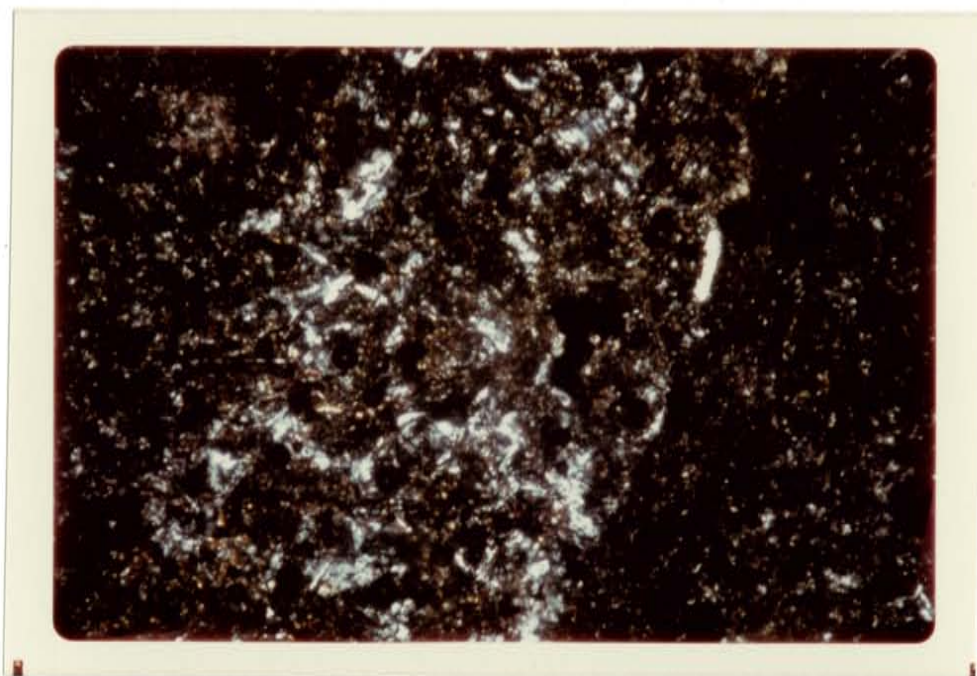
The border facies is the only dike rock that contains magnetite-hematite crystals in thin veinlets and joint planes. Plate 3. Intratelluric magnetite and hematite crystals are absent in this facies, but are abundant in all other facies. Compositional characteristics are shown in tables I, II, III, and fig. 2, (samples 76, 77). Plagioclase determinations reveal the existence of two plagioclases, the more sodic type is probably due to recrystallization under the influence of hydrothermal solutions.

The outer-intermediate hornblendic facies of the diorite dike has a high percentage of ferromagnesian minerals, mainly hornblende and augite, with typically coarse texture (sample 72). The hornblende crystals are large with lengths commonly reaching 3 mm. or more and plagioclase of An<sub>36</sub> composition. In the field the rock is strongly sheared and under the microscope it is highly altered. Pink dikes, about 10 cm. in thickness, which have a cross-cutting relationship with the main dike, were noted in the outer-intermediate zone.



Plate 1: Mottled border facies of the diorite dike. Tongues of more massive texture are also present. The mottled rock has recrystallized under the influence of hydrothermal solutions which leached Ca, Mg, and Ti and deposited Na, K, Si, and Al. Two plagioclases are present, one andesine and the other albite. Note also the light color of the rock.

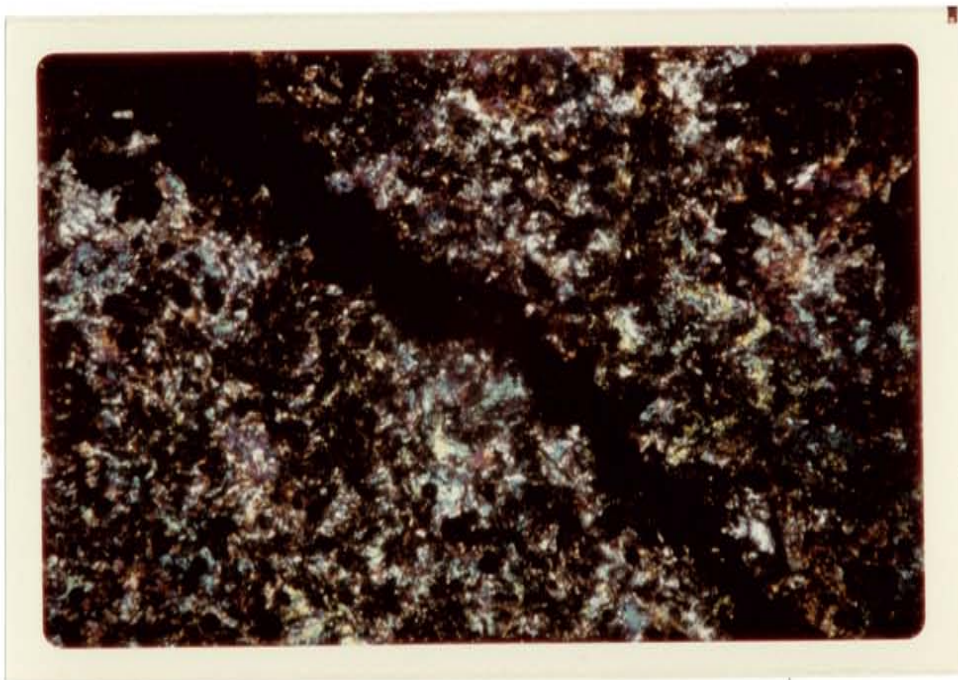




0.5 mm



Plate 2: Photomicrograph of the mottled border facies of the diorite dike showing textural differences. The lighter-colored area in the center has developed a coarser texture by recrystallization and is enriched in felsic minerals as a result of addition of Na, K, Si, and Al.



0.5 mm

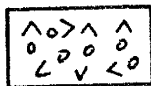


Plate 3: Photomicrograph showing hydrothermal vein of magnetite and hematite in the mottled border facies of the diorite dike. The birefringent material is mainly epidotized pyroxene and amphiboles with interstitial plagioclase. The matrix of the rock is depleted in iron. (x nicols)

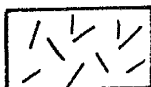
Symbols and abbreviations for figure 2.



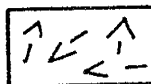
J-17, 182: Iron mineralization



76, 77: Mottled border facies



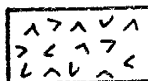
71, 156: Central facies



157: Inner-intermediate pyroxenic facies



72: Outer-intermediate hornblendic facies



83: Diabase sills

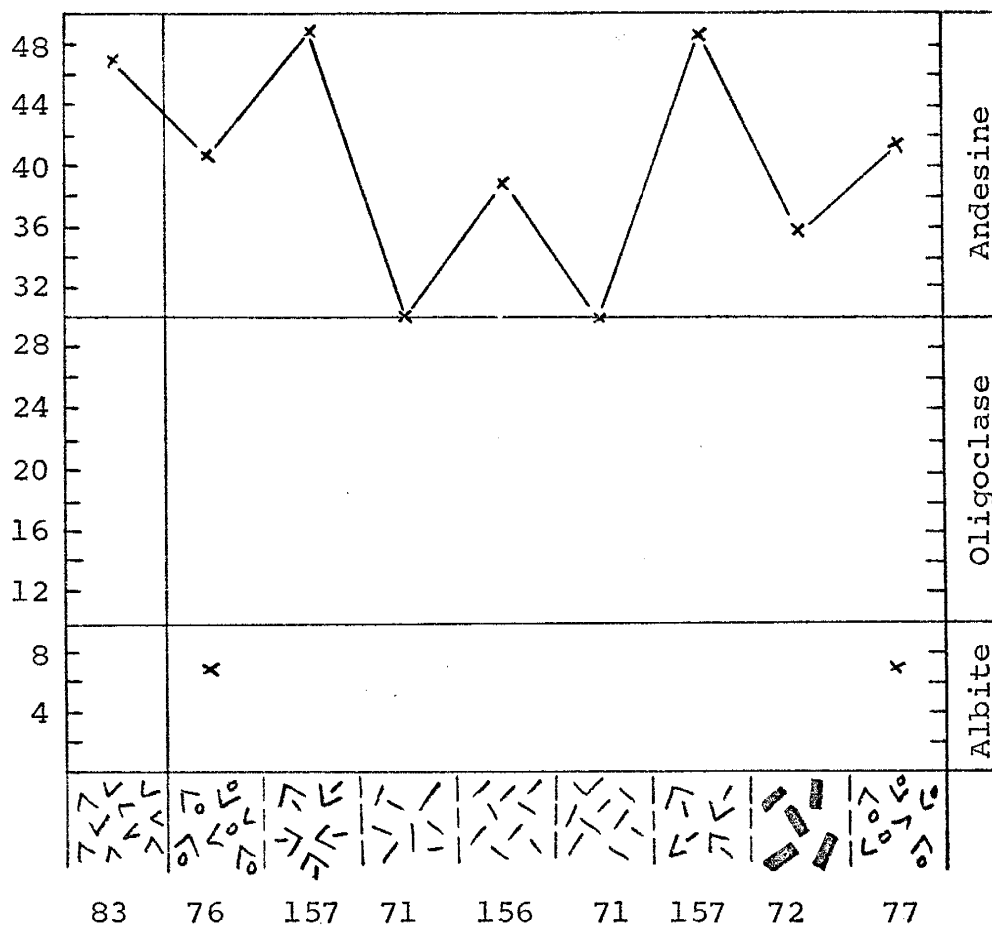


Figure 2.- Variations in plagioclase composition in diabase sills and diorite facies. Note two plagioclases in the mottled border facies due to albitization by hydrothermal fluids.

These thin dikes contain xenoliths of the outer-intermediate facies and are compositionally similar to the central dike facies, except that the plagioclase is of albitic composition (sample 73). Plate 4.

The inner-intermediate pyroxenic facies has a coarse texture and a high percentage of ferromagnesian minerals. It differs from the outer-intermediate facies by a general predominance of pyroxene over amphibole. The grain size is smaller, with the ferromagnesian minerals having a maximum size of about 1 mm. This facies possesses more massive characteristics, although extensive zones of epidotization and kaolinitization have been recognized (sample 157).

The central quartz-dioritic facies can be subdivided into two subfacies recognizable by different characteristics in the field. They are a gray-green, feldspathic, equigranular, diorite subfacies; and a cream porphyritic quartz diorite subfacies which contains more quartz, potassium feldspar and hornblende at the expense of plagioclase and pyroxene. Although these two subfacies have some differences in mineralogical composition (samples 71, 156, table I) their chemical compositions are similar (table III). Their textural differences are due to variation in the rate of cooling with pockets of the cream porphyritic subfacies scattered within the gray-green equigranular subfacies giving the



Plate 4: Thin, pink aplitic dike intruding the outer-intermediate hornblende facies of the diorite dike. Alteration along the contact gives the illusion of chilled margins against the aplite dike.

illusion of xenoliths. Plate 5. The cream porphyritic subfacies with its coarser texture and higher concentrations of silica, soda, and potash constitutes the center of the composite dike and represents the most highly differentiated material (note figs. 6 and 8).

#### Contact Silicate Minerals

The contact metasomatic minerals present in Jones Camp area are tremolite, actinolite, epidote, andradite, cordierite talc and acmite. Optical properties were used to identify the minerals according to the characteristics described by Kerr (1959); x-ray diffraction data were used to confirm the identifications. Tremolite-actinolite in columnar, fibrous, or asbestiform aggregates are the principal metasomatic minerals and in general account for more than 80% of the metamorphic minerals present. Plate 7, 8, and 9.

Tremolite-actinolite is distinguished from talc by the characteristic extinction angles in longitudinal sections and by x-ray parameters. Cordierite and andradite, noted in petrographic studies, were confirmed by x-ray diffraction techniques. Plate 8 and 9. Acmite could not be distinguished under the microscope; its existence was established by x-ray analysis.

Development of the contact minerals depended upon tem-

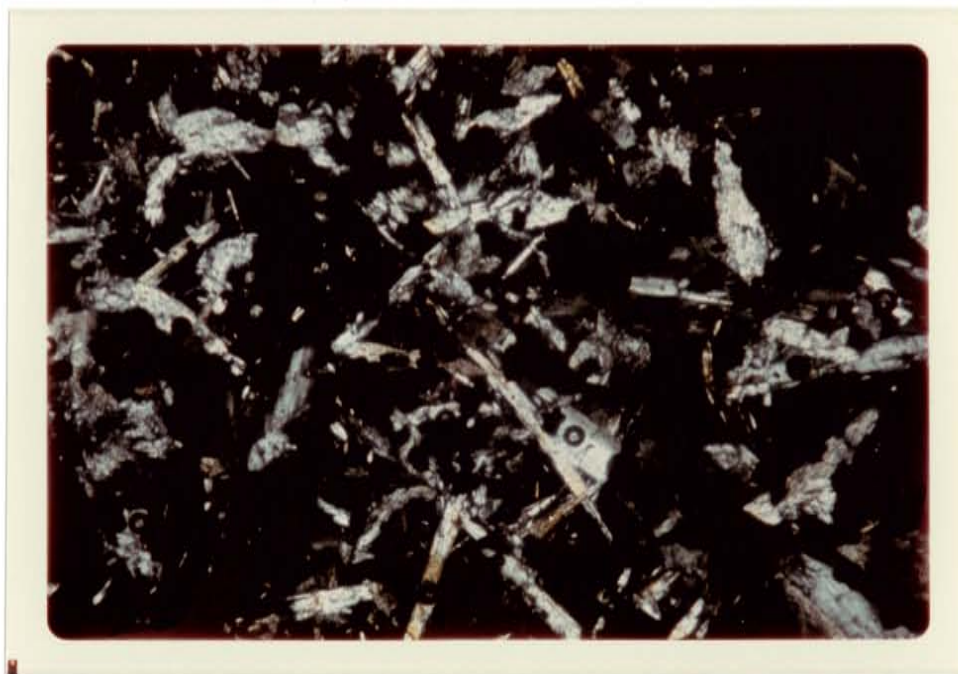


Plate 5: Pseudo-xenolith of the cream, k-feldspar-quartz-hornblende, porphyritic subfacies in the gray-green, feldspathic, equigranular subfacies of the central facies of the diorite dike. The structure is believed to result from concentration of volatiles which depress the freezing point and allow a coarser textured rock to crystallize.





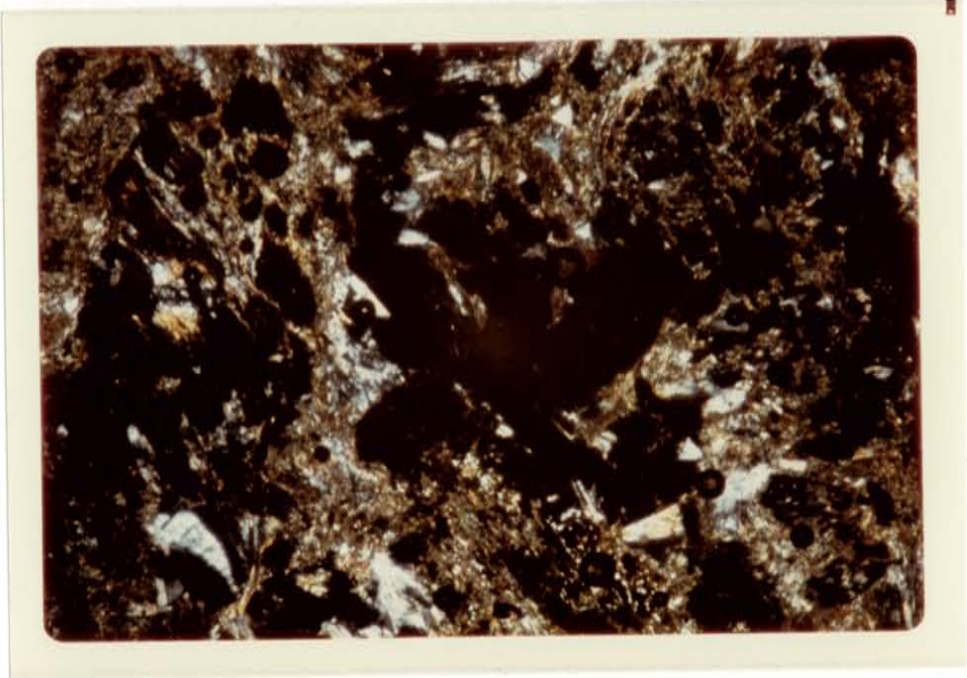
Plate 6: Panoramic view of the west boundary of the mapped area looking north. The diorite dike trends W-NW and forms the ridge at the center of the picture. The water gap in the ridge provided exposures for sampling a cross-section of the dike. (section D-D, geologic map) In the background, the San Andres Formation dips gently away from the dike. Soft gypsum beds of the Yeso Formation form the valley in the foreground.



0.5 mm



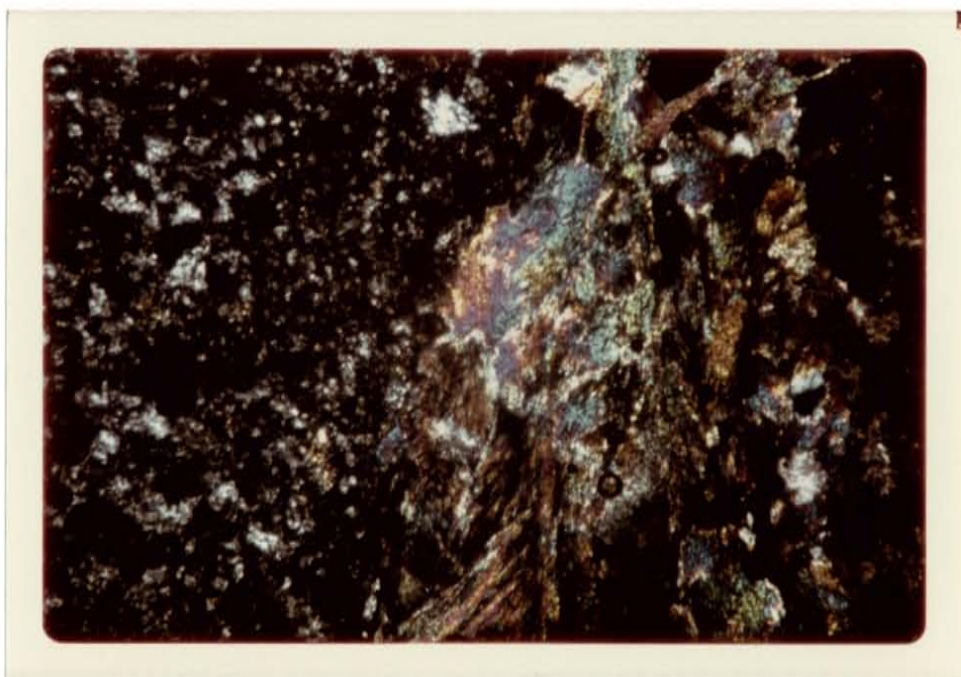
Plate 7: Photomicrograph showing twinned, prismatic crystals of actinolite-tremolite intergrowth with magnetite and hematite. (x nicols)



0.5 mm



Plate 8: Photomicrograph showing andradite garnet (black) intergrown with asbestiform actinolite-tremolite in the contact zone. The grayish-white minerals are plagioclase and quartz. (x nicols)



0.5 mm



Plate 9: Photomicrograph showing cordierite (gray mineral on left) and actinolite-tremolite. Patches of epidote are visible in the actinolite-tremolite. (x nicols)

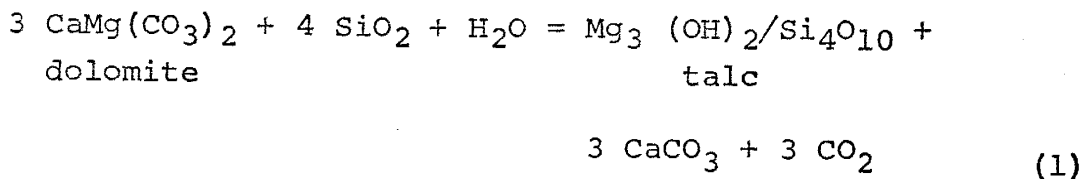
perature, pressure, hydrothermal fluids and the composition of the host rocks. Heat was furnished mainly by the intrusive body, and pressure controlled by the depth of burial. Water and  $\text{CO}_2$  were the dominant chemical reactants. In general if carbonates and water or hydroxyl-bearing minerals occur in metamorphic reactions,  $\text{CO}_2$  and  $\text{H}_2\text{O}$  are liberated. The smaller the amount of  $\text{CO}_2$  and  $\text{H}_2\text{O}$  incorporated in the contact minerals, the higher the temperature of metamorphism (Winkler, 1967). Water is very important in approaching thermodynamic equilibrium during mineral paragenesis. Kaliseva (1970) states that the phase rule characteristics of solid-state reactions in dry systems are not obeyed under hydrothermal conditions.

Although Winkler (1967) mentions that metamorphism is essentially an isochemical process, the author is skeptical of this idea with respect to contact metasomatic areas. The aureole of contact metamorphism is immediately adjacent to the intrusive and the addition and removal of constituents is inescapable.

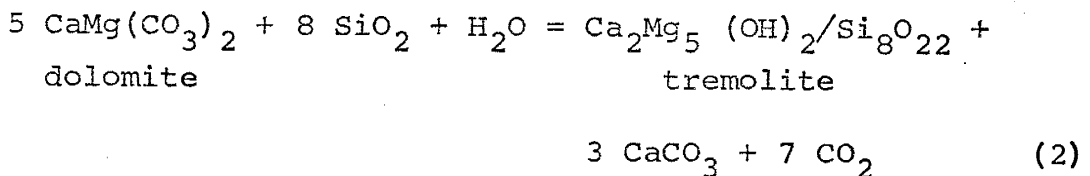
Metamorphic associations in the deposit define contact metamorphic conditions of the albite-epidote-hornfels facies characterized by low temperature and very low fluid pressures of generally less than 1500 bars (Winkler, 1967, p. 19).

Figure 3, represents the albite-epidote-hornfels facies on an ACF diagram. The lines of chlorite and tremolite-actinolite are variable depending upon their composition.

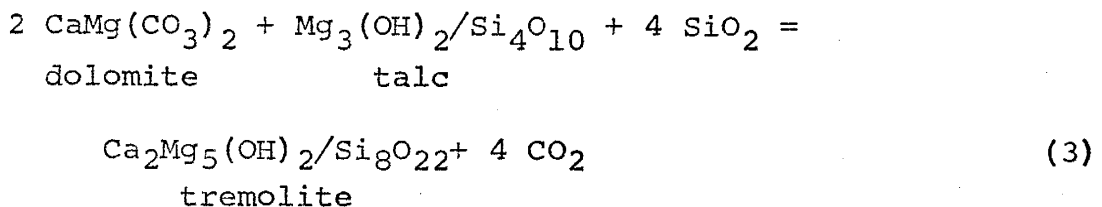
The formation of talc (identified by C.T. Smith) in siliceous dolomite involves the following reaction:



A common reaction for the formation of tremolite is:



Since talc is present in only minor amounts and because talc first become stable at temperatures bellow tremolite stability reaction (1) can probably be rewritten as:



Since the Yeso limestones are dolomitic but non-siliceous, application of the experimentally derived equations to the deposit requires an additional source of silica. Sandstone intervals could have furnished the necessary silica. Better development of the contact minerals is observed where this supply is present (northern and central portions of the map

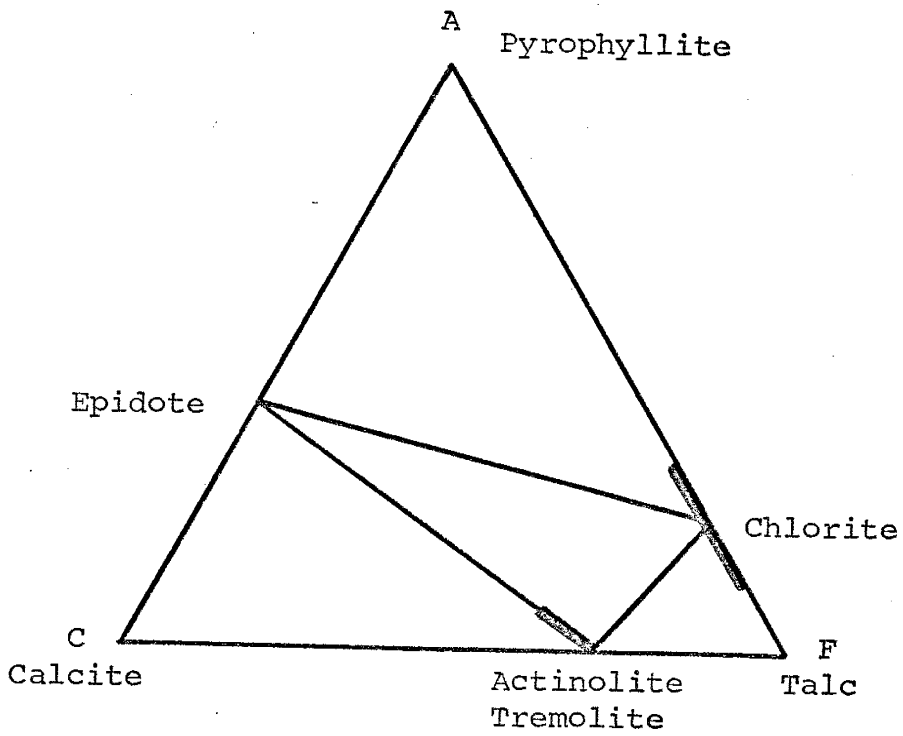


Figure 3.- Albite-epidote-hornfels facies  
(After Winkler, 1967)

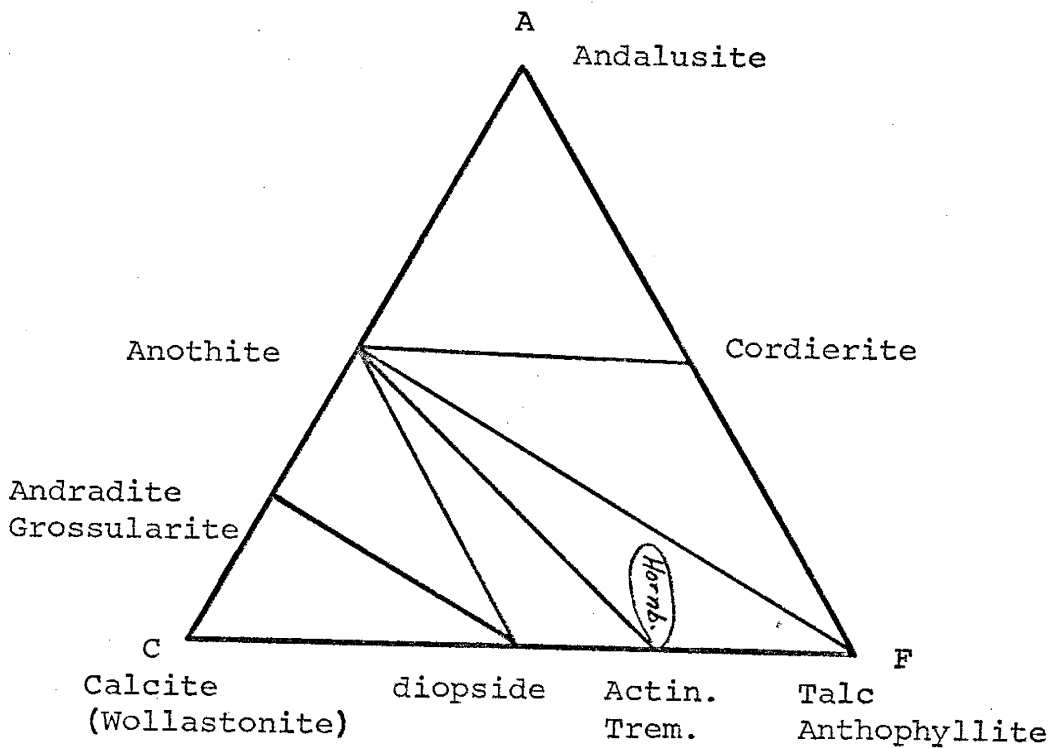
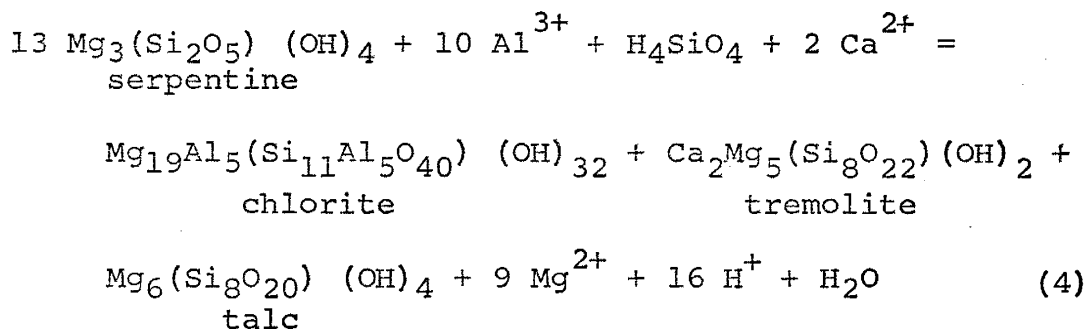


Figure 4.- Hornblende-hornfels facies  
(After Winkler, 1967)

area).

Curtis and Brown (1969), studying ultrabasic bodies in Unst, Shetland, find that with serpentine (excess of MgO) available equation (4) accounts for the mineral assemblage in contact metamorphosed diabases present at Jones Camp. The diabases contain enough MgO (see table III), thus the chlorite, tremolite, talc assemblage is expectable by similar reaction:



In this equation the formation of actinolite has not been considered, but with the addition of  $\text{Fe}^{2+}$  to the left side of the reaction and the replacing of some of the  $\text{Mg}^{2+}$  of the talc and tremolite by  $\text{Fe}^{2+}$  and  $\text{Ca}^{2+}$  actinolite will result.

The presence of cordierite in some reaction products indicates that the contact metasomatism in these areas reached the lower limit of the hornblende-hornfels facies (represented in fig. 4, after Winkler, 1967).

Current understanding of amphibole paragenesis is exceedingly limited because of the inherent complexities



of the problem (Ernst, 1968). Laboratory studies are complicated by the variations in chemical composition of amphiboles and slow reaction rates.

### Ore Minerals

Polished sections were made of six of the ore specimens. Magnetite and hematite are the principal ore minerals. Intermingled grains of magnetite and specular hematite indicate concurrent formation. The proportions between magnetite and hematite are generally in the ratio 3-4:1. Pyrite crystals in minor amounts commonly surround and fill spaces between grains of magnetite and hematite, indicating a later period of formation. Small concentrations of goethite occur in microveins, patches, and aureoles surrounding the hematite-magnetite crystals.

Abundant, well developed cubic crystals of pyrite have been observed with the iron oxides in some of the gypsum gangue. Plate 10. Sulphur ions supplied by the gypsum beds are probably responsible for the abnormal pyrite concentration in these mineralized bodies. Reaction between sulphur and the iron supplied by the mineralizing solutions could produce the assemblage by the following reaction:

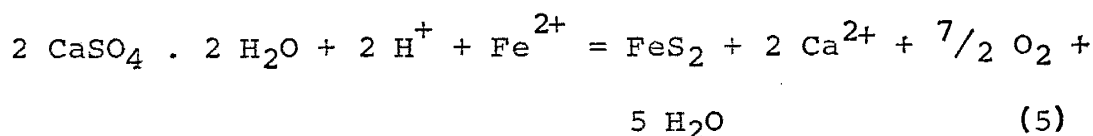




Plate 10: Close up between mineralized and barren disseminated magnetite-hematite is visible (blue-gray) below the contact; nearby pure white gypsum is visible in the upper right hand corner. Limonite from oxidized pyrite has stained the contact yellow. Pyrite is not very abundant in the Jones Camp deposits and occurs primarily in gypsum beds where minor amounts of sulfide ion may have been formed by reduction of calcium sulfate.

Some copper carbonate fracture coatings and chalcocite mineralization were observed in the field. No copper minerals were observed in the polished samples of the ore.

## GEOCHEMISTRY

### CHEMICAL ANALYSES OF ROCKS AND ORES

The chemical analyses shown in table III, were plotted on a  $(\text{SiO}_2) - (\text{Na}_2\text{O} + \text{K}_2\text{O} + \text{Al}_2\text{O}_3 + \text{Fe}_2\text{O}_3) - (\text{MgO} + \text{CaO} + \text{FeO})$  triangular diagram and compared with published analyses of similar rocks. The classification of Nockolds (1954) indicates a dioritic classification for the dike rocks (fig.5), this classification is in agreement with classification tables by Travis (1955).

Chemical changes of major oxides and some minor elements across contacts between diabase sills, different facies of the dioritic dike and the ore bodies are represented in a composite section (figs. 6 and 7). The order of crystallization of the diorite facies is also shown in figure 8. The composite diorite dike, the main intrusive of the area, has been subdivided into four facies which can be recognized in the field by textural, structural and mineralogical variations. The reasons for subdividing the dike into four different facies of the same dike instead of into individual dikes are:

- 1) the consistent change in chemical composition of the

Table III

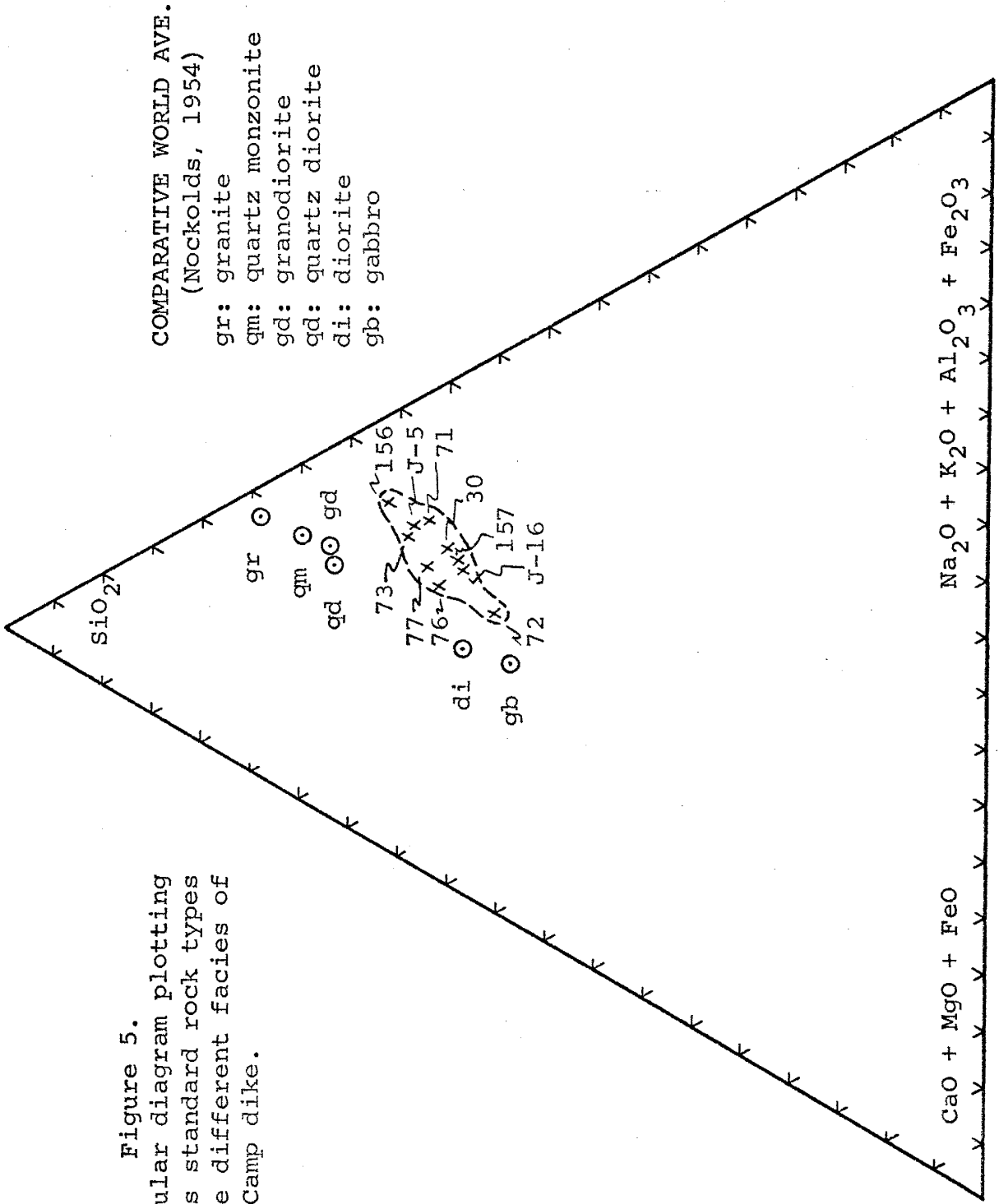
## Chemical Analyses of Igneous Rocks and mineralization bodies. (%)

| Sample | SiO <sub>2</sub> | Al <sub>2</sub> O <sub>3</sub> | CaO   | K <sub>2</sub> O | Fe <sub>2</sub> O <sub>3</sub> | MgO  | Na <sub>2</sub> O | TiO <sub>2</sub> | Zn* | Sr* | S*  |
|--------|------------------|--------------------------------|-------|------------------|--------------------------------|------|-------------------|------------------|-----|-----|-----|
| J-5    | 62.96            | 14.62                          | 6.18  | 3.82             | 5.65                           | 2.28 | 8.18              | 1.32             | 147 | 349 | 456 |
| 76     | 59.86            | 14.66                          | 8.09  | 2.31             | 4.67                           | 3.59 | 6.33              | 1.39             | 149 | 455 | 450 |
| 83     | 55.56            | 13.47                          | 7.19  | 0.96             | 8.11                           | 6.66 | 5.26              | 1.97             | 168 | 358 | 365 |
| 30     | 57.72            | 13.88                          | 8.50  | 4.74             | 6.50                           | 2.39 | 5.87              | 1.67             | 139 | 354 | 445 |
| 73     | 64.20            | 15.25                          | 7.08  | 1.24             | 4.63                           | 2.74 | 9.90              | 0.56             | 155 | 318 | 391 |
| 71     | 62.28            | 14.77                          | 7.29  | 2.64             | 5.66                           | 1.91 | 9.53              | 1.30             | 150 | 342 | 463 |
| 72     | 50.87            | 14.81                          | 11.48 | 1.59             | 6.41                           | 5.26 | 3.41              | 2.26             | 143 | 333 | 450 |
| 156    | 67.83            | 14.62                          | 4.53  | 2.78             | 5.80                           | 1.44 | 10.97             | 1.50             | 151 | 373 | 472 |
| 157    | 57.13            | 14.23                          | 8.43  | 2.72             | 8.88                           | 3.02 | 5.83              | 1.90             | 132 | 319 | 448 |
| **182  | 4.95             | 11.94                          | 12.76 | 0.26             | 28.07                          | 5.62 | 6.78              | 0.25             | 97  | 139 | 352 |
| 77     | 60.87            | 14.49                          | 8.42  | 1.53             | 4.44                           | 4.24 | 8.13              | 0.99             | 153 | 358 | 446 |
| J-16   | 57.90            | 14.88                          | 8.92  | 2.78             | 8.26                           | 4.02 | 5.57              | 1.38             | 137 | 292 | 334 |
| **J-17 | 4.75             | 11.85                          | 12.48 | 0.27             | 28.00                          | 4.56 | 6.46              | 0.19             | 99  | 132 | 340 |

\* p.p.m.

\*\* Mineralized samples; the total weight percent of the ore samples is low because Ca was calculated as CaO being probably CaCO<sub>3</sub>. Percentages of Fe<sub>2</sub>O<sub>3</sub> are well below the real values, due to lack of proper standards available.

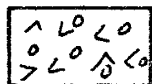
Figure 5.  
 Triangular diagram plotting  
 various standard rock types  
 and the different facies of  
 Jones Camp dike.



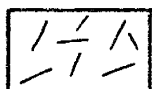
Symbols and abbreviations for figures 6 and 7.



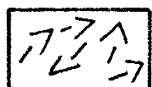
J-17, 182: Iron mineralization



76, 77: Mottled border facies



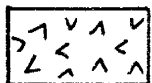
71, 156: Central facies



157: Inner-intermediate pyroxenic facies



72: Outer-intermediate hornblendic facies



83: Diabase sills

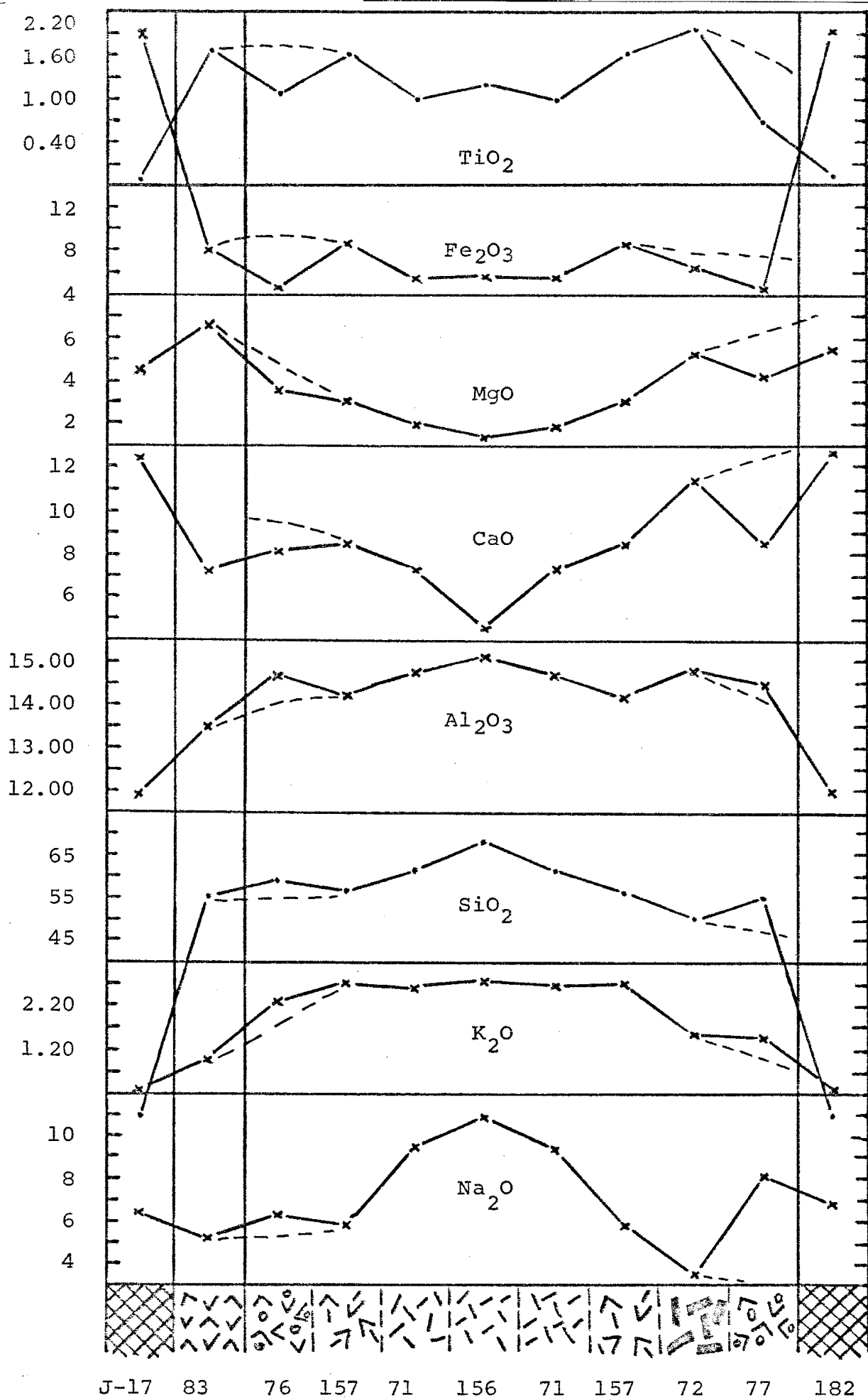


Figure 6.- Chemical changes of major elements across contacts between iron bodies, diabase sills and diorite facies. The dotted curves represent the original compositional trends before alteration of the mottled border facies.



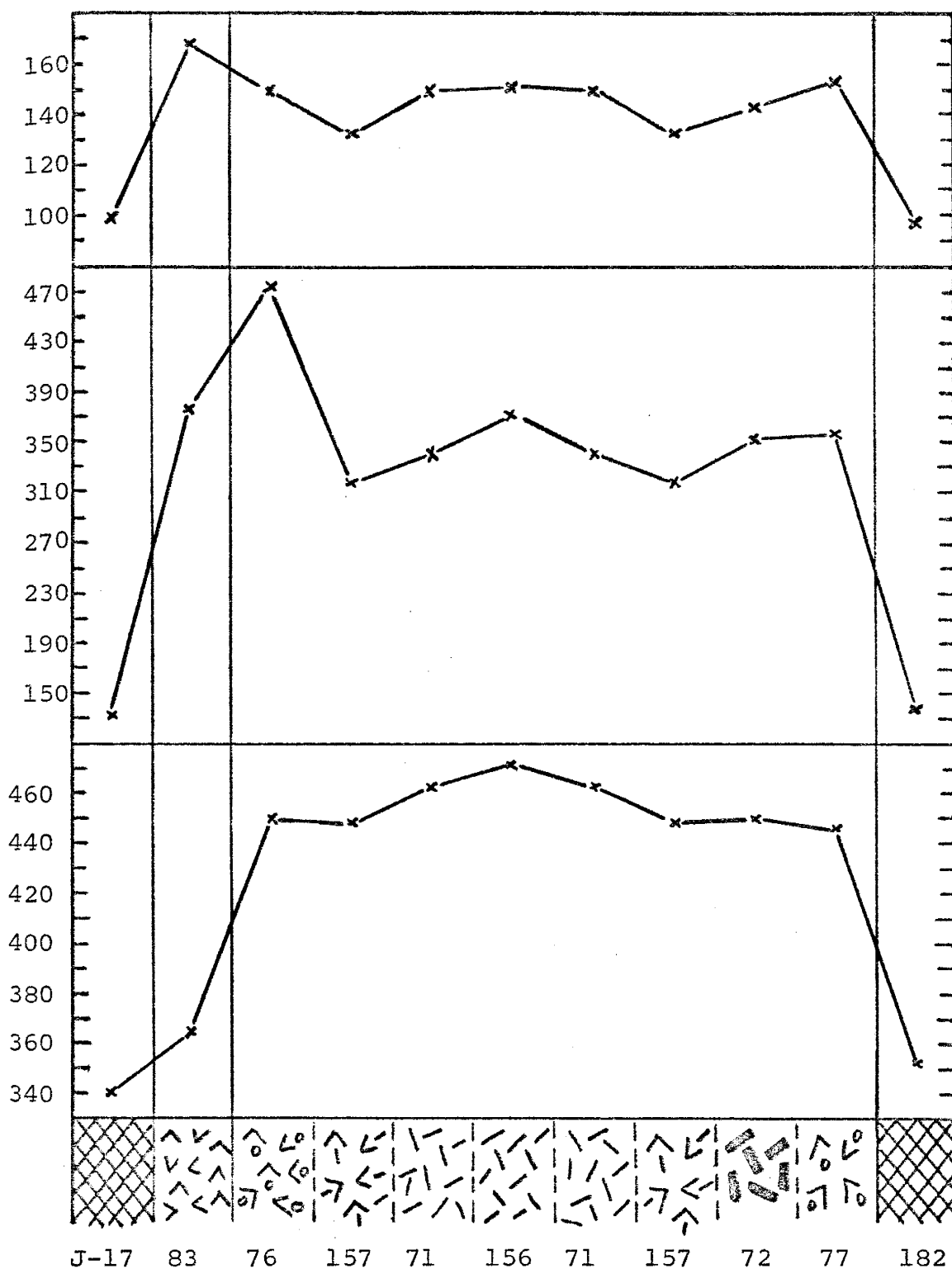


Figure 7.- Chemical changes of minor elements across contacts between iron bodies, diabase sills, and diorite facies. (Composite section)

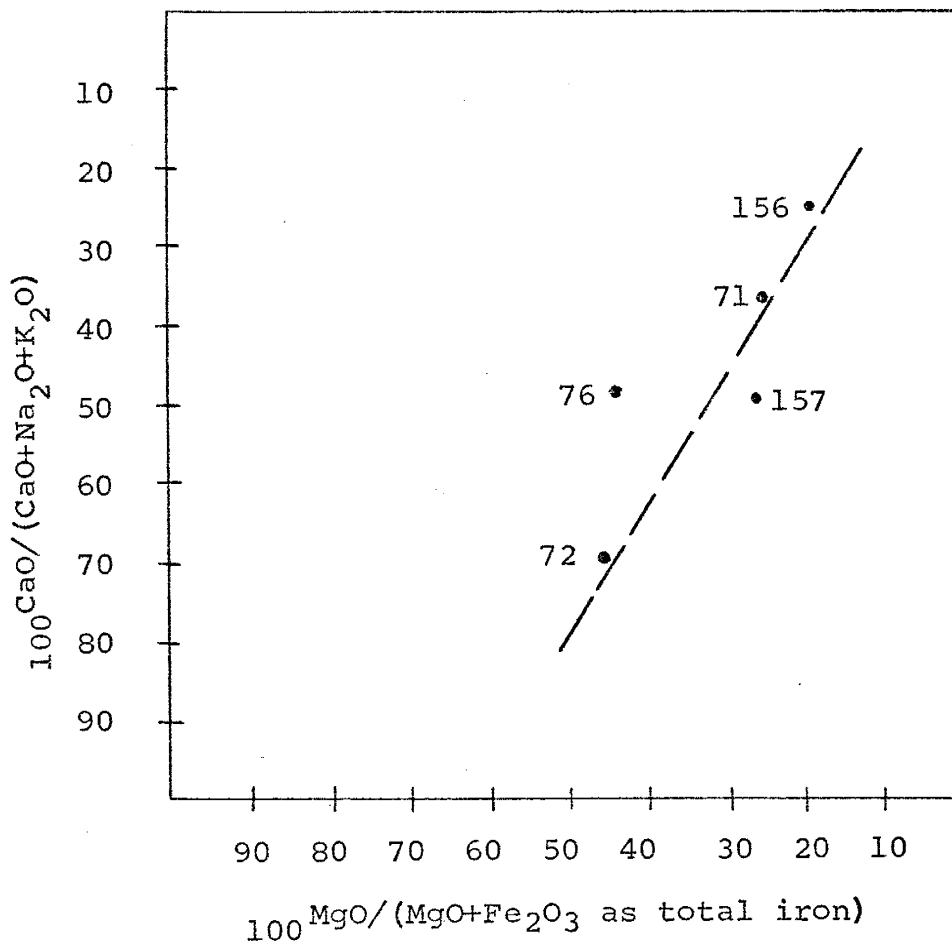


Figure 8.- Diagram of lime-alkalies and magnesium-iron ratios. The straight line represents Nockolds' average (1954) for igneous rocks. The numbers represent samples from the principal facies of the Jones Camp diorite. Upper points reflect later stage of crystallization.

dike according to normal differentiation (more basic toward the borders, more acidic toward the center).

2) the lack of crosscutting relationships between the different facies

3) the absence of xenoliths of previously emplaced dikes. Differences in volatile content towards the central part of the dike give the impression of a different facies or xenoliths of one dike in other. These pseudo-xenoliths are segregation pockets of the same rock which were rich in volatiles and thus crystallized more slowly and developed a coarser texture.

4) the lack of chilled margins between the various facies.

5) the apparent gradational contacts between the facies.

6) symmetrical repetition of the dike facies on opposite sides of the center.

Higher concentrations of  $\text{CaO}$ ,  $\text{MgO}$ ,  $\text{Fe}_2\text{O}_3$  (as total iron) and  $\text{TiO}_2$  are found in the marginal facies (except for the recrystallized mottled border facies) as opposed to higher concentrations of  $\text{SiO}_2$ ,  $\text{Na}_2\text{O}$ , and  $\text{K}_2\text{O}$  toward the central facies;  $\text{Al}_2\text{O}_3$  behaves rather uniformly as expected.

The apparently abnormal chemical behavior displayed by the mottled border facies appears to represent the effects of hydrothermal solutions rising along the dike margins causing

partial recrystallization (the mottled texture), leaching of some elements, and enrichment of others. This would explain the higher concentrations of  $\text{SiO}_2$ ,  $\text{Na}_2\text{O}$ , and possibly  $\text{Al}_2\text{O}_3$  in the mottled border facies in comparison to the intermediate facies. The depletion of  $\text{Fe}_2\text{O}_3$ ,  $\text{TiO}_2$ , and possibly  $\text{CaO}$  in the mottled border facies is also understandable by this model. The patterns followed by the three minor elements are difficult to interpret. Sr shows a marked concentration in the mottled border facies and is least abundant in the pyroxenic intermediate facies; Zn is most abundant in diabases, and least abundant in the pyroxenic intermediate facies. Sulphur is most abundant in the central facies and least abundant in the diabases.

#### ESTIMATED CONDITIONS OF ORE FORMATION

In order to characterize the conditions of ore deposition, the author has calculated the bounding temperatures, pressure, and gas fugacities which would permit the deposit to form.

##### Confining Pressure

An estimation of the confining pressure during contact metasomatism and ore deposition can be made from the depth

of intrusion of the adjacent dike. Following Buddington's criteria for granite emplacement, the dike seems to belong to the epizone type which extends from the surface to a depth of about six miles.

Criteria of epizone emplacement are:

- 1) the discordance of the dike,
- 2) unmetamorphosed country rock outside the contact metamorphic zone,
- 3) association of low grade contact metasomatism with the intrusion,
- 4) common miarolitic texture of the dike rock,
- 5) the deformation of country rock as result of forceful intrusion, and
- 6) the massive character of the dike rocks.

Reasons for believing the dike to be of Tertiary age were cited earlier. Lindgren (1933) suggests that toward the end of the Cretaceous period practically all of New Mexico was covered by a sedimentary mantle 6,000 to 9,000 feet thick. Sedimentary cover of at least 3500 feet existed in the area by the time of intrusion, according to regional stratigraphic studies (Wilpolt and Wanek, 1952). So, an estimation of depth of diorite emplacement between one and two kilometers seems reasonable, indicating confining pressures between 250

and 500 bars.

### Temperature of the Dioritic Dike

The melting temperature of an igneous rock is dependent upon several variables. The most important of these variables are rock composition and water vapor pressure.

Assuming that the melting temperature of an igneous rock, at constant water pressure, will vary linearly with silica content of the rock, figure 9 was constructed (after Yoder and Tilley, 1962) which shows the relationship between water pressure and melting temperature for a diorite with the same composition as the average dike rock at Jones Camp.

If the average dike rock at Jones Camp were saturated

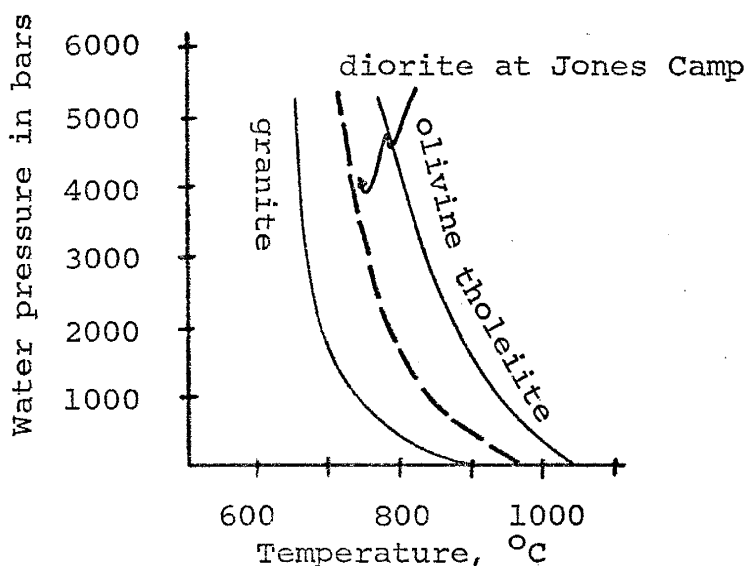


Figure 9.- Beginning-of-melting curves of granite and olivine tholeiite. (From Yoder and Tilley, 1962).

with water, then the water pressure of the magma would be in the range of 500 to 1000 bars which is about double the estimated above. However, the stratigraphic thickness used in this estimate is a minimum and probably establishes the lower limit of pressure. The presence of amphiboles in the dike confirms the higher water pressures. Pyroxenes in mafic magmas (Yoder and Tilley, 1962) are only stable at water pressures lower than 1000 bars, at higher water pressures amphibole is formed. The existence of abundant hornblende, not only in the central parts, but also toward the margin of the dike, indicate that the upper limit of water pressure in the magma was higher than 1000 bars and was perhaps as high as 1500 bars. This does not appreciably alter the melting temperature of the dike rock as can be seen in figure 9. Variation from 500 to 1500 bars water pressure will only produce a change of  $80^{\circ}\text{C}$ ; thus, the magma probably had a temperature between 800 and  $900^{\circ}\text{C}$  during the time of the dike intrusion.

#### Temperatures of Formation of Contact Metamorphic Minerals

The contact metasomatic minerals were developed at a somewhat lower temperature than the intrusive rock. The temperature of intrusion will limit the maximum temperature

of contact metasomatism; however, some other criteria must be used to determine the lower temperature limit. The contacts of the main intrusive are generally with silica-free limestones or low-silica diabases which complicate the interpretation of the contact assemblages. The silica free limestones and diabases are poor indicators of contact metasomatic effects (Winkler, 1967, p. 34).

Using an intermediate composition for the diorite dike in figure 10, indicates that the country rock reached a temperature of about  $600^{\circ}\text{C}$  (also see Fyfe and others, 1958, fig. 107).

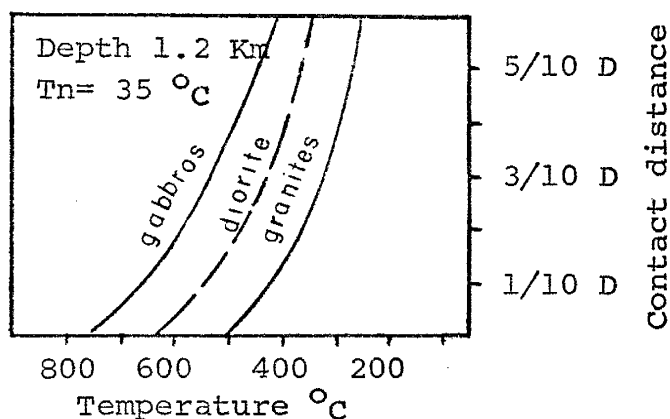


Figure 10.- Heating of the country rock adjacent to the intrusive.

D: thickness of the intrusive

$T_n$ : temperature of the country rock by depth of burial. (After Winkler, 1967).



Experimentally determined stability relations of the existing metasomatic minerals also establishes temperature limits on the contact metamorphism. Tremolite-actinolite assemblages are by far the most abundant. Assemblages of tremolite-actinolite, epidote, plus or minus chlorite limit the metamorphic minerals to the albite-epidote-hornfels facies and indicate temperature between 500 and 530°C for 0.5 to 1.5 kilobars (Winkler, 1967, fig. 13).

Isobaric equilibria involving tremolite-actinolite and the composition of the fluid phase of  $\text{CO}_2 + \text{H}_2\text{O}$  (fig. 11, after Winkler, 1967), have been determined by Greenwood (1962), Mets and Winkler (1964), and Ernst (1967, figs. 26, 27). The tremolite has a stability range of 425 to 525°C at 1000 bars, depending upon the mole fraction of  $\text{H}_2\text{O}$  and  $\text{CO}_2$  in the fluid phase. Since a higher mole concentration of  $\text{H}_2\text{O}$  than  $\text{CO}_2$  can be inferred (Brown, 1970), the tremolite temperature of formation must be closer to the lower limit. This lower limit is probably 450°C or at least less than the 480°C at which a water rich-fluid phase starts to form wollastonite. Wollastonite is never found in rocks metamorphosed at the relatively low temperatures of 400-500°C, not even in contact metamorphic rocks formed at shallow depths and corresponding pressures of only a few hundred bars

(Winkler, 1967, pag.35). Even if the temperature and pressure were favorable for the formation of wollastonite, the formation of tremolite would liberate enough  $\text{CO}_2$  so that the formation of wollastonite would have occurred at a higher temperature than existed in the contact (Winkler, 1967, fig. 6, Greenwood, 1962). Finally, the upper stability limit of tremolite has been determined by Boyd (1959) and reproduced

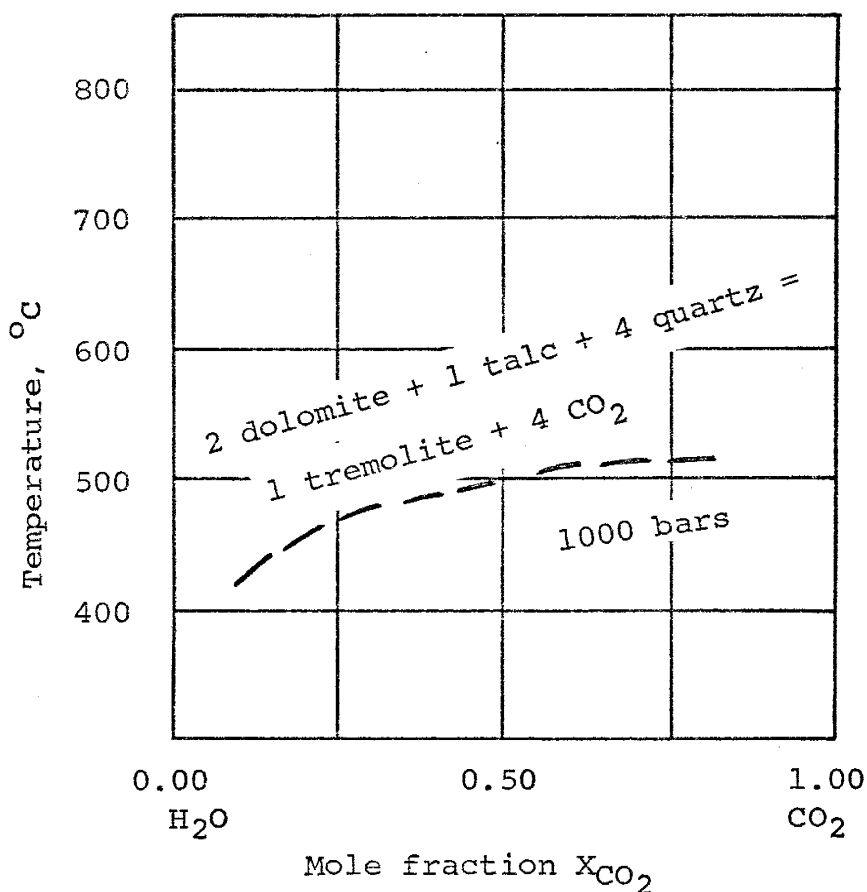
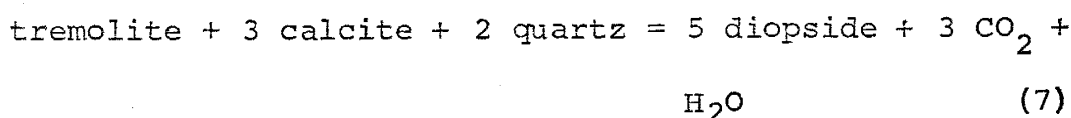
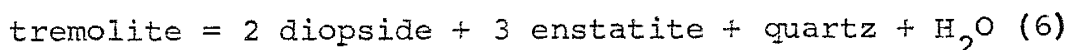
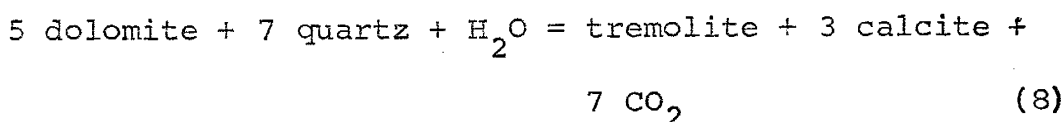


Figure 11.- Possible isobaric equilibrium of tremolite reaction.  $X_{\text{CO}_2}$  is the mole fraction of  $\text{CO}_2$  in the fluid phase consisting of  $\text{CO}_2 + \text{H}_2\text{O}$ .

by Ernst (1967, fig. 25) as 800-840°C for 500-1000 bars of fluid pressure. At higher temperatures enstatite and diopside take the place of tremolite as shown in the following reactions:



Reaction for the formation of tremolite is:



Increase in the partial pressure of CO<sub>2</sub> from the previous reaction prevented the formation of wollastonite at the temperature of the deposit.

Presence of the pyroxene acmite, not only in the metasomatic rocks, but also in the mottled border facies, indicates broad ranges of temperature at any fluid pressure.

The association of hematite, magnetite, quartz and acmite has been determined experimentally by Ernst (1962) at 2000 bars; the temperature of formation of this assemblage is quite dependent on the fugacity of oxygen. If oxygen fugacities of the order of  $10^{-15}$  and  $10^{-18.2}$  are used, then the temperatures of 520 and 650°C are determined from the equilibrium assemblage.

The presence of cordierite in local areas along the contact indicates temperatures of 510 to 530°C and the beginning of the hornblende-hornfels facies. Cordierite is an important mineral for use in temperature estimation because of its negligible temperature variation at different fluid pressures.

Garnet is also present in the contact areas. Although it constitutes only small percentage of the contact metasomatic minerals, its presence contributes to the estimation of the contact temperatures. Ernst (1967, fig. 37) indicates temperatures of 500 to 575°C for the association magnetite-garnet at 2000 bars and with oxygen fugacities of  $10^{-15}$  to  $10^{-18}$  (also see oxygen pressure determinations). Similar data extrapolated from its fig. 30 determines temperatures of 480 and 620°C at 3000 bars for the assemblage hematite + quartz + andradite + fluid and magnetite + quartz + andradite + fluid. Experimental studies of Gilbert (1966) and Ernst (1966) indicate that a constant temperature and fluid pressure garnet-rich rock would appear more frequently at relatively high oxidation states and hornblende rich rocks, at lower oxidation states. The absence of hornblende in the contact metasomatic rocks and the presence of andradite with tremolite in areas of abundant miarolitic cavities in

the dike rocks indicates moderately oxidizing conditions. Thermodynamic calculations by Zharikov (1970, fig. 126) determine temperatures between 500 and 550°C at 1000 bars for the formation of pyroxene-garnet assemblage.

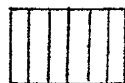
Epidote is a widespread contact metasomatic mineral and is generally the last calcium silicate to form at Jones Camp. It coats joints and fractures extensively in the border facies and shear zones of the diorite dike. The temperature of formation of epidote is estimated to be 400°C at 1 atmosphere (Stringham, 1952). At 1000 bars, the upper stability limit of epidote is 480°C (Merrin, 1960). Calculations by Zharikov (1970) have determined temperatures of 400 to 450°C for the assemblage pyroxene-epidote.

Figure 12, summarizes the contact minerals temperature relationship. The author believes that the circled area between 480-550°C represents the temperature of formation of the contact metasomatic minerals. Six lines of evidence out of ten fall in this area in which the most diagnostic metasomatic minerals, cordierite, actinolite, tremolite, and epidote are present.

Figure 12.- Temperatures and pressures of contact minerals found at Jones Camp deposit, estimated from published experimental data.



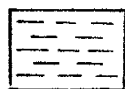
- \*(1) Actinolite-tremolite, epidote + chlorite  
500-530°C ----- 500-1500 bars. (Winkler, 1967).



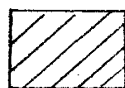
- \*(2) Tremolite ----- 425-525°C ----- 1000 bars.  
(Figure 11, Winkler, 1967).



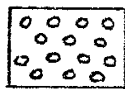
- (3) Actinolite ----- 450-850°C ----- 500-1000 bars.  
(Ernst, 1967).



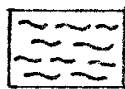
- (4) Magnetite-hematite, quartz, actinolite -----  
520-650°C ----- 2000 bars. (Ernst, 1962).



- \*(5) Cordierite ----- 510-530°C ----- 500-1500 bars.  
(Winkler, 1967).



- (6) Magnetite, garnet ----- 500-575°C ----- 2000 bars.  
(Ernst, 1967).



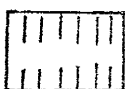
- (7) Magnetite-hematite, quartz, andradite, fluid.  
480-620°C ----- 3000 bars. (Ernst, 1967).



- (8) Pyroxene, garnet ----- 500-550°C ----- 1000 bars.  
(Zharikov, 1970).

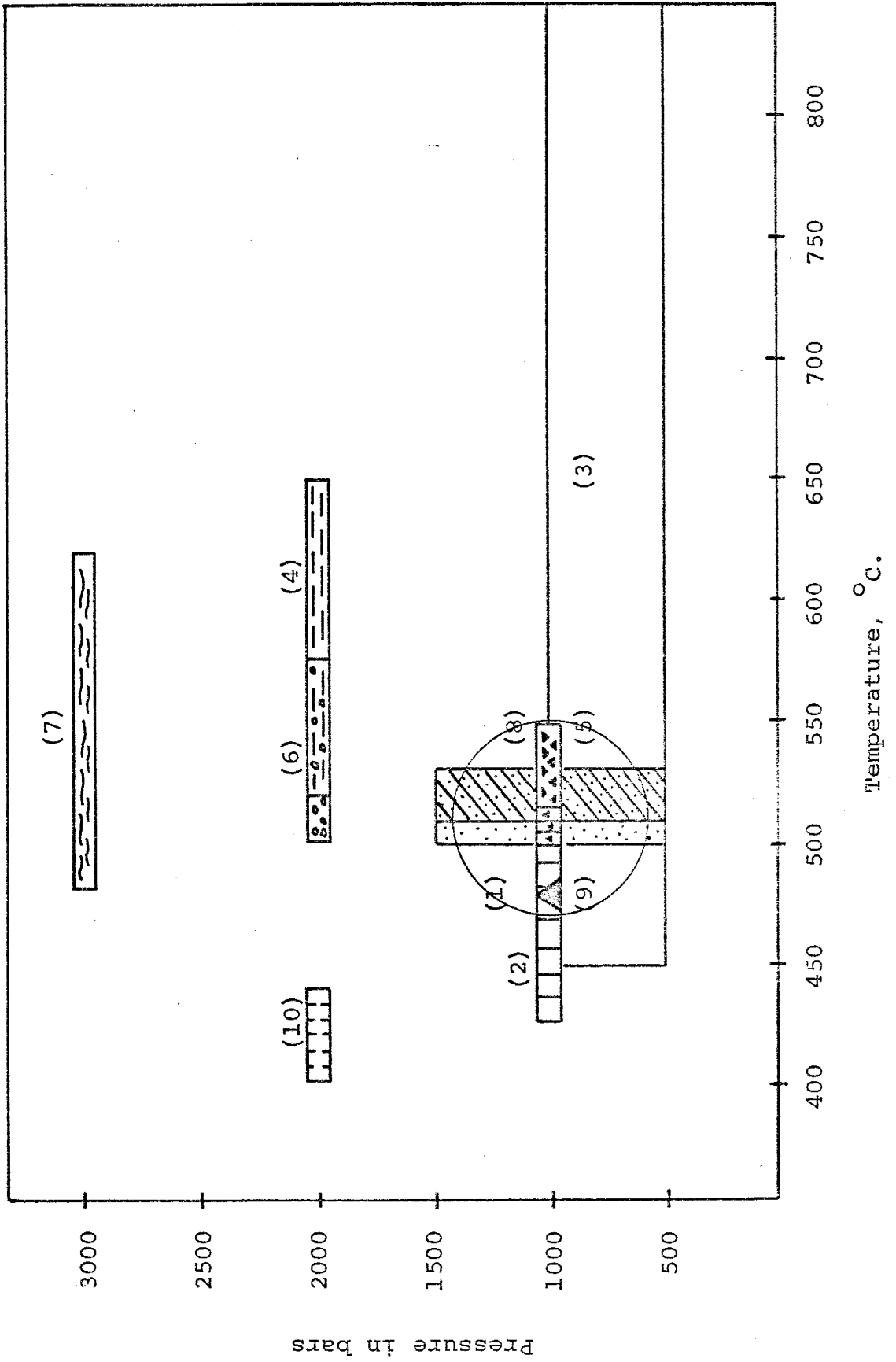


- \*(9) Epidote ----- 480°C ----- 1000 bars. (Merrin,  
1960).



- (10) Epidote, pyroxene ----- 400-450°C ----- 2000 bars.  
(Zharikov, 1970).

\* Minerals abundant at Jones Camp and whose presence is considered especially diagnostic of temperature and pressure conditions.



### Temperature of Formation of Ore Minerals

The metallic minerals present in the ore bodies are magnetite, hematite, pyrite and negligible amounts of goethite. Pyrite was deposited either at the same time or later than magnetite-hematite. The metallic minerals were generally deposited later than, or more or less simultaneously with, the contact silicate minerals. The contact silicate minerals limit the upper temperature of formation of the ore minerals. Since the metallic mineral assemblage cannot be used to reliably estimate temperature of formation of the ore minerals, oxygen fugacities (see section on oxygen pressure) and experimental data will be used to check estimated temperatures.

The reaction:



constitutes an oxygen-buffer system. The previous discussion of contact metamorphic minerals suggested an average temperature of formation of about 480 to 550°C. Using a recent compilation of thermodynamic data (Robie and Waldbaum, 1968), the equilibrium value for the fugacity of oxygen at 527°C was calculated to be  $10^{-16.2}$ . Oxygen fugacities of  $10^{-18.2}$  to  $10^{-15.2}$  calculated on page , and plotted in figure 13, indicate temperatures between 500 and 590°C for the magnetite-



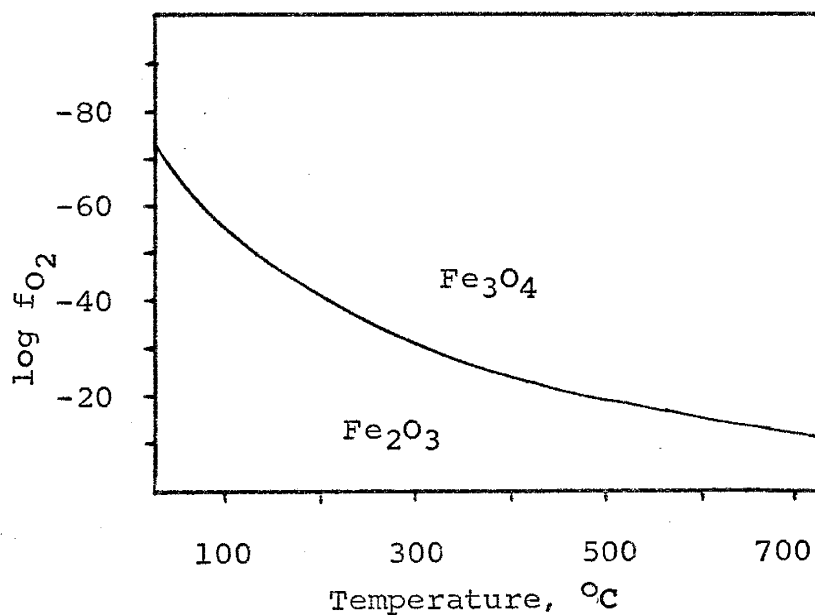


Figure 13.- Stability field of iron oxides in the Fe-O system. (After Holland, 1959)

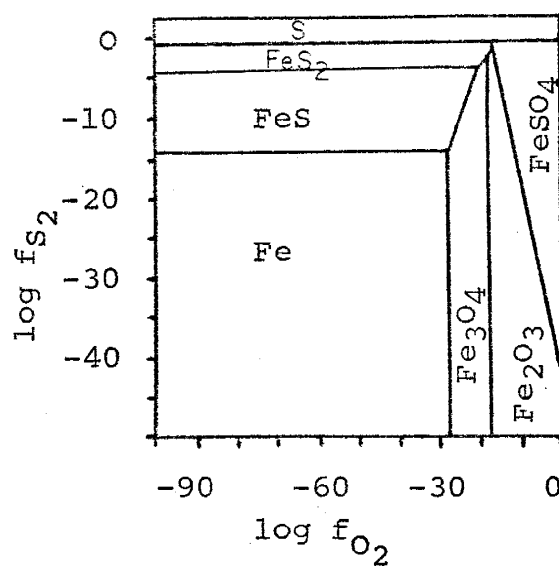


Figure 14.- Isothermal diagram at 527 °C, through the  $\log f_{O_2}$ - $\log f_{S_2}$ -T, in the Fe-O-S system. (After Holland, 1959).

hematite association. The upper limit is questionable since wustite is a stable iron mineral above  $560^{\circ}\text{C}$  and is not present in the deposit (Barnes and Kullerud, 1961, p. 669). Also, this temperature is definitely higher than temperatures shown by the associated contact silicate minerals. Experimental studies by Martin and Piwinskii (1969) demonstrate the possibility of the movement of iron in aqueous vapor phase and its subsequent deposition as specular hematite at temperatures of  $450$  to  $580^{\circ}\text{C}$ . Experimental deposition of magnetite, hematite, feldspar, and quartz in particular zones was also observed to occur between temperatures of  $470$  to  $515^{\circ}\text{C}$ . These experimental assemblages are consistent with those observed in Jones Camp deposits. The matrix of the border facies of the diorite dike is markedly depleted in iron indicating a strong possibility of leaching of iron by a water-rich vapor of magmatic origin escaping through the border zones. A similar mechanism was envisioned by Mackin (1968) for the Iron Springs district of Utah.

In summary, the presence of abundant specular hematite in miarolitic cavities of the dike close to the marginal zones (samples 30 to 36) indicates a temperature of formation of at least  $450^{\circ}\text{C}$  and more probably  $580^{\circ}\text{C}$  (Martin and

Piwinskii, 1969, p. 802). The presence of thin, late-stage veins of magnetite, hematite, feldspar and quartz toward the border zones of the intrusive, indicates a temperature of formation between 470 and 515°C for the assemblage (Martin and Piwinskii, 1969, p. 800).

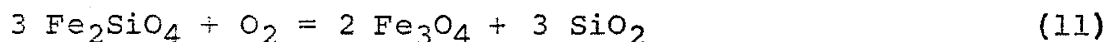
#### Oxygen Pressure in the Ore-forming Fluid

The partial pressure of O<sub>2</sub> plays an important role not only in the determination of the temperature limits of the contact silicate minerals, but also in the temperature and compositional ranges of the metallic minerals. The amount of free oxygen in the vapor phase is best defined by the oxidation states of iron (Krauskopf, 1957).

The common iron oxide minerals near igneous contacts are magnetite-hematite and ferrous silicates; therefore, oxygen fugacity should be in equilibrium according to the reactions (10) and (11). The approximate temperature of the country rock at the igneous contact is 600°C



$$G_{600^\circ} = -30.2 \text{ kcal}; \quad \log. K = 7.6$$



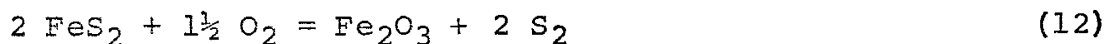
$$G_{600^\circ} = -73.0 \text{ kcal}; \quad \log. K = 18.2$$

Reaction (10) is the formation of hematite from magnetite;

reaction (11) is the formation of magnetite from fayalite. The equilibrium concentrations of oxygen are  $10^{-15.2}$  atmospheres for equation (10) and  $10^{-18.2}$  atmospheres for equation (11). The figure  $10^{-15.2}$  is presumably a reasonable upper limit and  $10^{-18.2}$ , a reasonable lower limit for the amount of free oxygen in most magmatic gases at  $600^{\circ}\text{C}$ . If  $10^{-15.2}$  is exceeded, then all the iron present should be converted to hematite (Krauskopf, 1957); and if free oxygen is less than  $10^{-18.2}$ , then fayalite will form (Holland, 1959).

#### Fugacity of Sulfur Species

Sulfur pressure may be calculated from the following reaction:



after Krauskopf's method (1957). Using data from Robie and Waldbaum (1968), the fugacity of  $\text{S}_2$  gas in equilibrium with the pyrite-hematite-magnetite assemblage at  $527^{\circ}\text{C}$  is  $10^{-1.4}$  atmospheres. This is not in agreement with older data (fig. 14).

Hydrogen sulfide gas may be formed by the reaction:



in order to calculate  $f_{\text{H}_2\text{S}}$  we must first establish a fugacity

value for  $H_2S$  gas. This may be done by considering the equation:



At  $527^\circ C$ , with water pressure of 1000 bars and oxygen fugacity of  $10^{-16.2}$  (required by the magnetite-hematite buffer), the fugacity of  $H_2$  gas is about  $10^{-5.5}$  atms.

Therefore the fugacity of  $H_2S$  under these conditions is  $10^{-2.7}$  atms. The equilibrium fugacity of  $SO_2$  may be calculated from the reaction:



At equilibrium,  $f_{SO_2}$  would be  $10^{-4.3}$  atmospheres.

The presence of anhydrite and the absence of wollastonite at Jones Camp implies that the  $f_{SO_2}$  must have been greater than  $10^{-4.3}$  atmospheres, but cannot be used to estimate how much greater it might have been. The presence of anhydrite in the deposit indicates higher oxidizing conditions than usual in the associated vapor (Krauskopf, 1957).

#### Fugacity of Carbon Dioxide

With the data available, the fugacity of carbon dioxide cannot be established with a  $f_{CO_2}$  buffer as was done for the oxygen and sulfur species. However, a first order approximation for the minimum value can be derived if we consider the interbedded sandstones to be capable of providing all of

the quartz needed for the reaction:



The absence of wollastonite in the contact metasomatic assemblage requires that  $f_{\text{CO}_2}$  was greater than the equilibrium value for the above reaction. The fugacity calculated for this reaction at  $527^\circ\text{C}$  is  $10^{2.37}$  atmospheres. Therefore, the fugacity of  $\text{CO}_2$  must have been greater than 232 atmospheres. The absence of siderite, for which thermodynamic data are very poor, provides an upper limit on  $f_{\text{CO}_2}$  of approximately  $10^3$  atmospheres for the conditions of interest. Assuming 1000 bars water pressure, this restricts  $\text{CO}_2$  to the range of from 232 to 1000 ( $10^{+2.37}$  to  $10^{+3}$ ) atmospheres.

## INTERPRETATIONS OF ORE GENESIS

### Sources of Iron

The iron in the deposits of Jones Camp, might have had any one of, or a combination of, the following sources:

- 1) Sedimentary rocks
- 2) Older diabases, and
- 3) Nearby dioritic intrusives.

### Sedimentary Rocks

In theory, the iron might have been leached from the

sedimentary rocks of the Yeso Formation. Since the limestones, gypsum, and sandstones of the formation are everywhere almost free of iron, extensive alteration of the sedimentary sequence might have occurred if some appreciable amount of iron were derived from them. Since this effect has not been noticed, this mechanism for the formation of the deposit is probably not possible.

#### Diabase Intrusives

Diabase bodies are extensively distributed in the area and at least two relative ages have been observed (point P). Since the diabase sills are unrelated spatially, their relative age is unknown. The diabase bodies, occurring spatially related to the dioritic dike, predate intrusion of the diorite.

Several features regarding the possible relationship of the diabase rocks and iron formation need to be mentioned:

- 1) The diabase rocks are very rich in iron, containing as much as 8% or more (sample 83, Chemical Analysis).
- 2) Massive iron deposits, a few of which are some distance from the diorite dike have been found inside diabase bodies. Drill holes have found mineralized bodies in diabase at depth.
- 3) Contact alteration between the diabase and iron

bodies within the diabase is lacking.

4) Iron bands are frequently observed in altered rock that was probably diabase originally. Plate 11.

5) Fluidal characteristics of hematite-magnetite bands in the diabase were observed.

6) Magnetite pseudomorphs were not observed, and non-selective replacement apparently occurred along favorable horizons.

Considering the above factors, it is believed that some planar, sheet-like iron bodies inside the diabase sills were emplaced with the diabase by some magmatic segregation process.

If some mechanism of lateral migration of iron could be invoked, then the possibility that the diabase could serve as a source of iron for the contact metasomatic deposits is an alternate hypothesis. The diabase bodies do not show evidence of extensive alteration. If they had been the iron source, then it would be expected that they would be bleached and presently poor in mafic constituents. The diabase is iron rich, therefore, the original "diabase" would have to have been extremely iron rich, almost peridotitic, to have provided the iron for the Jones Camp deposit. Chemical analyses show enrichment of Na, K,





Plate 11: Close up of rhythmic banding of magnetite-hematite in altered diabase. Crystal settling during cooling of the diabase sill probably accounts for the banding.

and Si relative to average diabase composition. It is thought that the late hydrothermal fluids associated with the diorite may have enriched the diabase in these components. Supporting evidence indicating that metals do not migrate toward contact aureoles is given by Barnes (1959) in the study of the contact metasomatic base metal deposits of Hanover, New Mexico.

#### Dioritic dike

Direct spatial relationship has been observed between the dioritic dike and the iron bodies which are generally situated in veins and pods parallel to the dike boundaries. Plate 12, 13, and 14. The parent magma which formed the dike was enriched in iron as indicated by the composition of the pyroxenic intermediate facies (table III, fig. 6). The border facies cannot be used to approximate the composition of the parent magma since it has recrystallized under the influence of hydrothermal fluids and is now a hybrid rock. Experimental studies of Hamilton, Burnham, and Osborne (1964) in basaltic melts under similar oxygen pressures have demonstrated that iron oxides crystallize at lower temperatures than the coexisting plagioclase and pyroxene. This agrees with paragenetic relationships observed at the Jones Camp dike, and suggest that iron



Plate 12: View looking E-SE along the boundary of the diorite dike showing iron mineralization in limestone and gypsum beds of the Yeso Formation. Most of the iron has been already mined. The brownish-white outcrops at the left side of the picture are gypsiferous sediments and alteration products at the contact of the diorite intrusive.

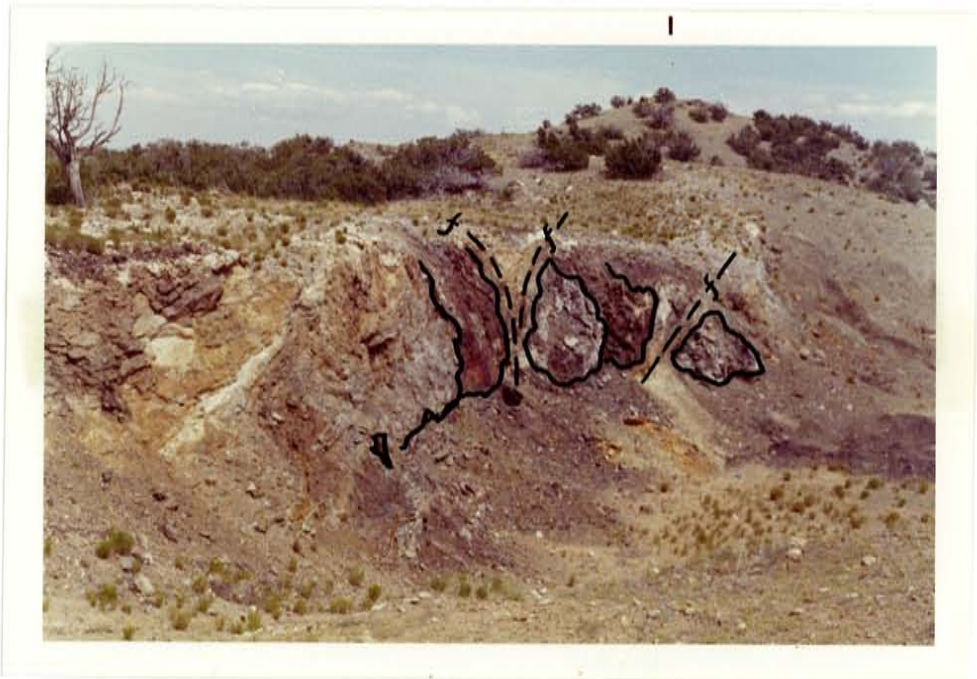


Plate 13: Contact metasomatic bodies of magnetite and hematite emplaced in faulted limestones of the Yeso Formation. The diorite dike is in the upper right corner of the photograph. See plate 14 for a close up of the fault visible at the right center.



Plate 14: Close up of fault zone cutting mineralized limestone. The magnetite and hematite replacements in limestones are evidenced by the dotted lines. The fault zone is unmineralized, apparently because of the unreactive breccia composed mainly of sandstone and gypsum.

would be concentrated residually for later transport in hydrothermal fluids. These hydrothermal fluids rising through the open spaces existing at the margin of the dike could not only deposit iron in joints and fractures, but also leach most of the iron present in the matrix of the mottled border facies and carry the iron toward a favorable place of deposition.

Experiments by Stanfield (1928) and Ovchinnikov (1959) also shed light on the formation of iron-rich segregations in dikes and plutons. They fused granite or basalt with limestone and upon gradual cooling the iron concentrated with the more silicic ions fraction. Metallic iron, magnetite, or hematite was formed depending upon the partial oxygen pressure used.

In summary, the writer believes that two mechanisms operated in the formation of the Jones Camp iron deposits. One was the formation of magnetite bodies together with diabase rocks in a process of magmatic segregation similar to those postulated by Lindgren (1933), Shand (1947), and Park and MacDiarmid (1970). The other and more important, accounting for almost all the valuable iron bodies present, was the formation of iron bodies due to the effects of residual hydrothermal iron-rich solutions differentiated

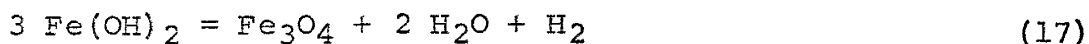
from the parent magma that emplaced the dioritic dike. These solutions probably became richer in iron by leaching iron from the pre-existing border facies. The iron was then deposited mainly in favorable reactive limestones of the Yeso Formation.

### Transportation of Iron

#### Magmatic Segregation

The formation of "magmatic" magnetite ores have been postulated by several authors, Kemp (1897), Spencer (1904), Bayley (1910), Colony (1923), Shand (1947), and Park and MacDiarmid (1970), etc. Park (1961, 1970) cites an example of magnetite-hematite ore magma in Laco Sur, Chile, and Shand discusses in detail the composition of similar magmatic metallic fluids. It is thought that in most deep magmas, ferrous oxide exceeds ferric oxide (3.08 % by weight of  $\text{Fe}_2\text{O}_3$  against 3.8 % FeO, Shand, 1947). In iron deposits in the crust  $\text{Fe}_2\text{O}_3$  exceeds the FeO indicating that some process of oxidation occurs later. Silicate minerals which crystallize early in basic magmas have much smaller FeO to MgO ratios than the magma as a whole. Since  $\text{Fe}^{++}$  and  $\text{Mg}^{++}$  occupy the same position in all of the early formed minerals, there must be a relative enrichment in FeO in the residual liquid along with soda, silica, water, and other soluble oxides

after formation of these early formed minerals. "Since the residual liquid has strong cations and weak silica-alumina anions, then the iron can only be present as a hydrosol of ferrous hydroxide peptized by the alkali (Shand, 1947)". Therefore, this ferrous hydroxide must be oxidized if it is the source of the magnetite. Possible atmospheric oxidation could occur in a extrusive magma but the main mechanism for intrusive magmas is one of self-oxidation:



The ferrous hydroxide loses water and the iron may be oxidized to magnetite; water and hydrogen escape while solid magnetite remains. The same mechanism was experimentally demonstrated by Berl and Von Taack (1928) with production of  $\text{Fe}_3\text{O}_4$  (89%), and  $\text{FeO}$  (10%) from heated ferrous hydroxide in the presence of water.

### Hydrothermal Fluids

Finding the composition of the ore-forming fluids is a challenge since different variables such as temperature, pressure, ionic species, and activity coefficients are involved and must be determined. Determination of these variables has to be based on the composition of the intrusives and the mineralogical associations of contact and ore minerals.

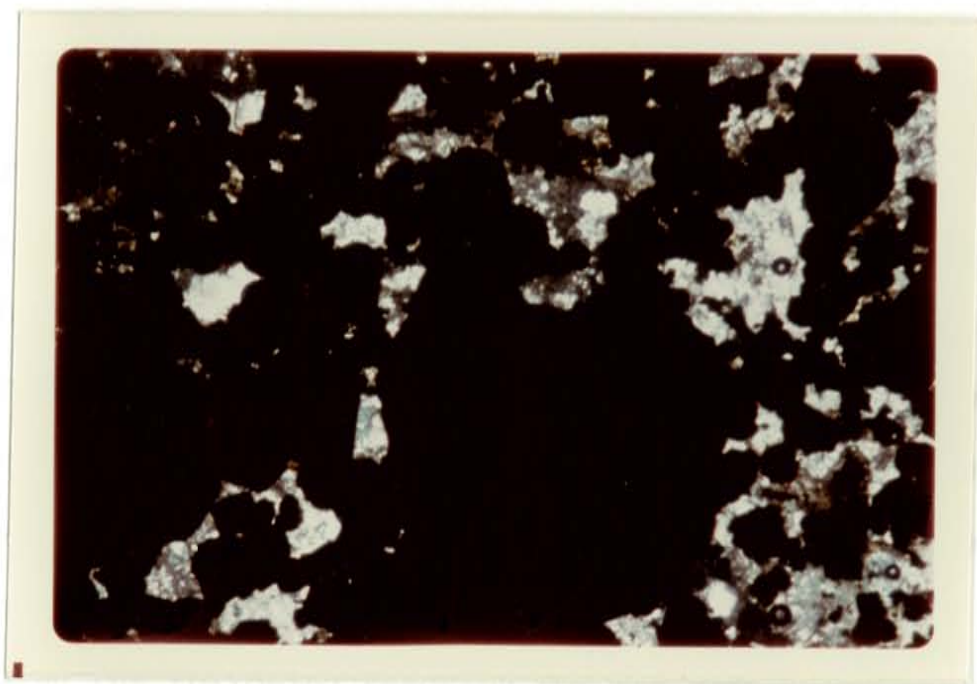


Even with full consideration given to all of the elements present, limitations arise from equilibrium factors and possible changes after deposition.

Osborne (1959) demonstrated that rocks of the calc-alkali trend are produced at constant partial oxygen pressure and, as water dissociates in the melt, the partial pressure of oxygen will either remain constant or increase slightly. The values of oxygen pressure used in this study are close to those used by Osborne, and are possible only in the presence of abundant water. Hamilton and others (1964) have established solubilities of water of 4.6 and 6.0 weight percent at  $1000^{\circ}\text{C}$  and 2000 bars in basalt and andesite. Kennedy (1955) has demonstrated that for every 0.5 weight percent increase of water there is a  $100^{\circ}\text{C}$  decrease in the melting temperature of the magma. Eight percent water at the contact of the intrusive body at approximately  $600^{\circ}\text{C}$  is sufficient to produce the hydrothermal activity observed in the area. The hydrothermal fluids, which escape mainly in the border zones of the igneous intrusives, will produce hydrothermal alteration and metallic deposition in the surrounding rocks ("contact metasomatism", Perry, 1969).

The water present in the system was at supercritical temperature. At a temperature of  $850^{\circ}\text{C}$  and a pressure of

2000 bars, the density of the aqueous fluid will be approximately half that of water under normal conditions (Smith, 1963). The presence of solutes like metal chlorides and gases like  $\text{CO}_2$  are especially important at limestone contacts, and are expected to change the pressure, volume, and temperature parameters of the system. Because of the replacement of considerable volumes of limestone by the hydrothermal fluid, the fluid composition and pH must have been such that calcite was unstable. Plate 15. The effects of temperature, pressure and salt dissolutions on the pH of water are considerable. The effects of pressure and salt dissolution can be considered small if compared to the effect of temperature. At a temperature of  $500^\circ\text{C}$  and a pressure of 2000 bars, the neutral pH of water will be 5 compared to 7 at the standard temperature of water (Barnes and Kullerud, 1961). Solubility of  $\text{CO}_2$  may be very high; Smith (1963) cites values of 20 weight percent at  $400^\circ\text{C}$  and 2300 bars. In the replacement of limestone by mineralizing fluids, considerable quantities of  $\text{CO}_2$  are released, greatly increasing the partial pressure of  $\text{CO}_2$ . The absence of siderite in the deposit limits the maximum possible  $f_{\text{CO}_2}$  since it appears to require in excess of  $10^3$  atmospheres to stabilize siderite at  $500^\circ\text{C}$  (Holland, 1959). The ratio of  $\text{CO}$  to  $\text{CO}_2$  at  $500^\circ\text{C}$ , in equi-



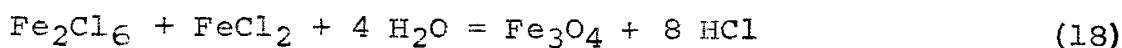
0.5 mm



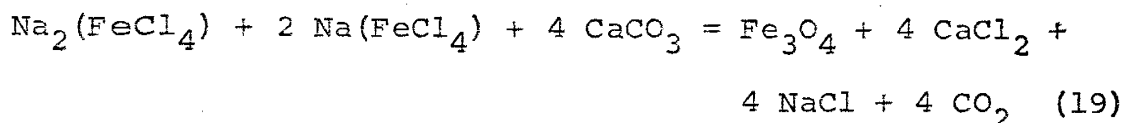
Plate 15: Photomicrograph showing incomplete magnetite and hematite replacement in limestone. The bluish-gray mineral is calcite. (x nicols)

librium with magnetite and hematite was determined to be 1 to  $10^7$  by Hawley and Robinson (1948); using the value of  $f_{\text{CO}}$  slightly greater than 200 atmospheres,  $f_{\text{CO}}$  was about  $10^{-4.52}$  atmospheres. For the assemblage magnetite-hematite, and pyrite, an oxygen fugacity of  $10^{-16.2}$  and a sulfur fugacity of  $10^{-1.4}$  atmospheres have been previously determined.

The addition of Fe, Si, Mg, Al, and Na, and the subtraction of Ca and  $\text{CO}_2$  in the zone of alteration are reflected by the contact minerals and the iron bodies. Several models for the transport of iron have been suggested not only by practical observation, but also by experimental data. Zeis (1929) postulated the following reaction for the formation of magnetite in the fumaroles of the Katmai area:



The HCl will be neutralized by limestones in the contact deposits permitting the deposition of  $\text{Fe}_3\text{O}_4$ . Kalnin (1962) suggested that iron could be in complex solutions according to the following reaction, where  $\text{FeCl}_4$  is a soluble complex noted in fluid inclusions by Smith (1954):



Thermodynamic calculations by Krauskopf (1957, 1964) indicate the impossibility of transporting iron in the form

of chloride by simple volatility. However, his statement that: "Volatility cannot be a general method of ore metal transportation but has a possible significance in the separation of metals from the magma and zones of high-grade metamorphism and perhaps in the deposition of some high-temperature ores (Krauskopf, 1964)" seems somewhat contradictory.

Geological observations of the iron deposits in the Urals and experimental work led Ovchinnikov (1960) to develop the concept of magmatogene ore genesis for deposits similar to those of Jones Camp. He suggested that these metals separate from the magma "by liquation caused by a change in the melt composition (interaction with limestone) or by a drop in temperature. The ore substances will be removed by gas bubbles in a process similar to froth flotation. Hydrothermal solutions of magmatic origin will migrate not only through the open fissures, but also through pore systems due to a filtration effect until they encounter a replaceable layer or zone (Ovchinnikov, 1960)".

Holser and Schneer (1961) calculated that at  $500^{\circ}\text{C}$  and 500 bars a concentration of 2.7 N HCl is necessary to transport 1 ppm of iron as  $\text{FeCl}_2$ ; however, Krauskopf (1957) estimated a concentration of only 0.06 N HCl in magmatic vapor at  $600^{\circ}\text{C}$ . Krauskopf's data is consistent with the

determinations of HCl concentrations of between 0.01 and 0.1 N in volcanic gases. It is not feasible to consider concentrations of HCl that could account for the mobilization of  $\text{Fe}_2\text{Cl}_6$  in gaseous form. It is quite possible that solubility plays a more important role than volatility in the mobility of iron chlorides because the solubility of  $\text{Fe}_2\text{Cl}_6$  is 5.350 grams per liter of water and  $\text{FeCl}_2$  is 1.050 grams per liter of water. Holser and Schneer (1961) emphasized that iron chloride compounds were in true solution and that iron chloride volatilities do not account for the mobilization of iron.

Recent experimental studies by Martin and Piwinskii (1969) with different types of rocks indicate that iron fractionates to a vapor phase between 1.25 and 10 kilobars. Experiments conducted on andesites and diabases indicate that iron was depleted in these rocks and that hematite crystals nucleated and grew at temperatures between 470 and 515°C. They also found zones of hematite + quartz + feldspar (Martin and Piwinskii, 1969, fig. 6) at temperatures between 470 and 515°C. This similarity with some hematite-magnetite-feldspar-quartz veins in the marginal zones of the Jones Camp intrusives indicates the feasibility of applying these experimental temperature determinations to Jones Camp.

The transportation of iron in a vapor phase is in agreement with the abundant specular hematite observed in miarolitic cavities of the diorite intrusive. Martin and Piwinski (1969) determined in their experiments with diabases that 6 percent of the total iron expressed as  $Fe_2O_3$  had been leached and transported toward cooler areas. "Volumetric calculations using this percentage could account for any sizeable contact iron deposit (Martin and Piwinski, 1969)".

In the Jones Camp deposit, the iron content of the mottled border facies, which has undergone hydrothermal alteration and iron leaching, is 40% less than the iron content of the diabases and the more basic facies of the dike (samples 83, 157, and 72). Conservative volumetric calculations (see appendix IV) indicate that the leaching of iron from the mottled border facies could easily account for a higher tonnage of iron than Kelley (1949) estimated for the reserves of the Jones Camp district. Additional calculations show that there was not enough water contained in the adjacent diorite dike, to transport the quantity of iron known in the deposit. Therefore, the rise of hydrothermal solutions along the borders of the dike appears necessary to leach and transport sufficient iron to form the deposits. These solutions may also have contributed

iron from a deep hydrothermal source, but such a source is not necessary.

### Deposition of Iron

#### Physical Controls

The great length, 9 to 10 miles (Kelley, 1949), and narrow width, 450 to 600 feet, of the main dioritic dike, seem to indicate emplacement of the igneous body in a previous fault zone. Geological studies have revealed brecciation along the contacts of the intrusive, but this phenomenon could also be accounted for by forceful intrusion. Later, mineralized fluids escaping through the fractured zones of the borders altered and replaced the chemically favorable rocks.

#### Chemical Controls

The limestones and calcareous gypsum beds were the major chemical factors controlling the mineralization. They helped to neutralize the ore-bearing solutions which formed the deposit.

Magmatic gases do not normally contain the large CO<sub>2</sub> content which must have existed in the supercritical fluids which altered the country rock and formed the ore deposits; the CO<sub>2</sub> content of the hydrothermal fluids was calculated



to be at least five times greater than would normally be expected (Krauskopf, 1957, p. 793). Therefore, these fluids probably were quite acid initially and far from equilibrium with calcite (the solutions were probably rich in NaCl and iron chlorides with a pH of 3 to 5). When the ore-bearing solutions reached a reactive medium (limestone) they were neutralized, depositing magnetite, hematite, and minor amounts of pyrite. As the pH of the solutions rose (from the carbonate ion uptake of hydrogen ion) with the dissolution of limestone, the stability of the iron oxide minerals increased.

## SUMMARY AND CONCLUSIONS

1) Diabase sills and a diorite dike were the intrusive rocks connected with iron mineralization. The diorite dike was subdivided into four facies of different structural, textural, and mineralogical characteristics. An increase in felsic minerals and Si, Al, Na, and K occur toward the central facies of the dike.

2) The ore bodies of massive magnetite-hematite had two origins. One was connected with the diabase sills in a process of magmatic segregation by crystal settling, and the other was connected with the rise of hydrothermal solutions along the border zones of the diorite intrusive. The hydrothermal deposits are larger and more numerous.

3) The altered and partially recrystallized border facies is depleted in Ca, Mg, Fe, and Ti, and enriched in Na, Al, and Si compared to the adjacent facies of the diorite dike. Leaching of 2% iron from the border facies by hydrothermal solutions could have provided more iron that is contained in the known reserves of the district. Even with the rather liberal assumptions of 8% water in the diorite magma and a solubility of 1000 ppm in the aqueous residual fluids, the

adjacent diorite dike could not provide sufficient fluids to account for the iron tonnages known in the deposit by a simple "sweating out" and lateral migration of fluids. Hydrothermal fluids rising along the dike borders are therefore necessary to do the work of leaching and transportation of iron.

4) Emplacement of the diorite dike occurred at shallow levels in the earths' crust, with initial temperature of 800-900°C and fluid pressures around 500-1500 bars. The approximate temperature of the intrusive at the contact with the country rock was 600°C.

5) Contact metasomatic minerals of the albite-epidote-hornfels facies and the begining of the hornblende-hornfels facies developed at the contact of the diorite intrusive, indicating temperatures between 475-550°C. These minerals include actinolite-tremolite, epidote, cordierite, andradite, talc, and acmite.

6) Magnetite and hematite were formed between 450-550°C under oxidizing conditions with oxygen fugacities of the order of  $10^{-15}$  to  $10^{-18}$  atms.  $S_2$  pressures were determined to be  $10^{-1.4}$  atms., fugacities of  $H_2S$  probably reached values of  $10^{-2.7}$  atms.,  $SO_2$  was determined to be greater than  $10^{-4.3}$  atms.

The fugacity of  $\text{CO}_2$  was calculated to be higher than  $10^{2.37}$  atms., and surely less than  $10^3$  atms.

7) The most favorable sites of mineral deposition were in the Yeso Formation at the contacts of the diorite dike with limestones and calcareous gypsum beds. Fractured and brecciated limestones adjacent to the igneous body provided both high permeability for the migration of the hydrothermal solutions and the neutralizing components to cause formation of the ore minerals.

## BIBLIOGRAPHY

- Ames, L.L., 1961, The metasomatic replacement of limestone by alkaline, fluoride-bearing solutions: *Econ. Geology*, v. 56, p. 730-739.
- Akella, J., and Winkler, H.G.F., 1966. Orthorhombic amphibole in some metamorphic reactions: *Contr. Min. Petrology*, v. 12, no. 1, p. 1-12.
- Alling, N.L., 1939, Metasomatic origin of the Adirondack magnetite deposits: *Econ. Geology*, v. 34, p. 141-172.
- Bain, W., 1936, Mechanism of metasomatism: *Econ. Geology*, v. 31, p. 505-535.
- Barnes, H.L., and Kullerud, G., 1961, Equilibria in sulphur containing aqueous solutions in the system Fe-S-O and their correlation during ore deposition: *Econ. Geology*, v. 56, p. 648-688.
- Barnes, H.L., 1959, The effect of metamorphism on metal distribution near base metal deposits: *Econ. Geology*, v. 54, p. 919-943.
- \_\_\_\_\_ 1967, *Geochemistry of hydrothermal ore deposits*: New York, Holt, Rinehart and Winston, Inc., 670 p.
- Barth, F.W., 1969, *Feldspars*: New York, Wiley-Interscience, 170 p.
- Barton, P.B., 1957, Some limitations on the possible composition of the ore forming fluid: *Econ. Geology*, v. 52, p. 333-353.
- \_\_\_\_\_ 1959, The chemical environment of ore deposition and the problem of low temperature ore transport, in *Researches in Geochemistry*: New York, John Wiley and Sons, Inc., 511 p.
- Bates, R.L., Wilpolt, R.H., MacAlpin, A.J., and Vorbe, J., 1947, *Geology of the Gran Quivira quadrangle, New Mexico*: New Mexico School of Mines, State Bureau of Mines and Min. Resources, Bull. 26, 55 p.

- Blondel, F., and Marvier, L., Publishers, 1952, Symposium sur les gisements de fer du monde: Internat. Geol. Cong., 19th, Algiers 1952, 593p.
- Boettcher, A.L., 1970, The system  $\text{CaO-Al}_2\text{O}_3\text{-SiO}_2\text{-H}_2\text{O}$  at high pressures and temperatures: *J. Petrology*, v. 11, no. 2, p. 337-379.
- Boyd, F.R., 1959, Hydrothermal investigation of amphiboles, in *Researches in Geochemistry*: New York, John Wiley and Sons, Inc., 511 p.
- Brown, T.H., 1970, Theoretical predictions of equilibria and mass transfer in the system  $\text{CaO-MgO-SiO}_2\text{-H}_2\text{O-CO}_2\text{-NaCl-HCl}$ : Unpublished Ph.D. thesis, Northwestern Univ., 136 p.
- Bowen, N.L., 1956, *The evolution of igneous rocks*: New York, Dover Publ., Inc., 332 p.
- Bowen, N.L., and Tuttle, O.F., 1949, The system  $\text{MgO-SiO}_2\text{-H}_2\text{O}$ : *Geol. Soc. America Bull.*, v.60, p. 439-460.
- Buddington, A.F., Fahey, J., and Vlisidia, A., 1955, Thermometric and petrogenetic significance of titaniferous magnetite: *Am. Journ. Sci.*, v. 253, p. 497-532.
- Butler, B.S., 1932, Influence of the replaced rock on the replacement minerals associated with ore deposits: *Econ. Geology*, v. 27, p. 1-24.
- Crawford, M.L., 1966, Composition of plagioclase and associated minerals in some schist from Vermont, U.S.A., and South Westland, New Zealand, with inferences about the peristerite solvus: *Contr. Mineral. and Petrology*, v. 13, p. 269-294.
- Curtis, C.D., and Brown, P.E., 1969, The metasomatic development of zoned ultrabasic bodies in Unst, Shetland: *Contr. Miner. and Petrology*, v. 24, p. 275-292.
- Darken, L.S., and Gurry, R.W., 1953, *Physical chemistry of metals*: New York, McGraw-Hill Book Co., 535p.
- Darton, N.H., 1917, A comparison of Paleozoic sections in Southern New Mexico, U.S. Geol. Survey, Prof. Paper 108-c, p. 31-55.

- Eastwood, G.E.P., 1965, Replacement on Vancouver island, British Columbia: *Econ. Geology*, v. 60, p. 124-148.
- Eckel, E.C., 1914, Iron ores, their occurrence, valuation, and control: New York, McGraw-Hill Book Co., 430 p.
- Edstron, J.O., 1953, The mechanism of reduction of iron oxides: *J. Iron Steel Institute*, v. 175, p. 289-304.
- Edwards, A.B., 1949, Natural exsolution intergrowths of magnetite and hematite: *Am. Mineralogist*, v. 34, p. 759-771.
- \_\_\_\_\_ 1954, Textures of ore minerals and their significance: Melbourne, Australasian Institute of Mining and Metallurgy, 242 p.
- Edward, P., 1947, Statistical relation between  $TiO_2$ ,  $Fe_2O_3$ , and  $FeO$  in rocks and ores during differentiation of a titaniferous magma: *Geol. Soc. America Bull.*, v. 58, no. 3, p. 197-210.
- Emmons, N.W., 1906, The Jones iron fields of New Mexico: *Mineralog. Mag.*, v. 13, p. 109-116.
- Flaschen, S.S., and Osborn, E.F., 1957, Studies of the system iron oxide-silica-water at low oxygen partial pressures: *Econ. Geology*, v. 52, p. 923-943.
- Fyfe, W.S., Turner, F.J., and Verhoogen, J., 1958, Metamorphic reactions and metamorphic facies: *Geol. Soc. of America, Memoir 73*, 259 p.
- Garrels, R.M., and Dreyer, R.M., 1952, Mechanism of limestone replacement at low temperatures and pressures: *Geol. Soc. America Bull.* 63, p. 325-379.
- Gilbert, M.C., 1966, Synthesis and stability relationships of ferropargasite: *Am. Jour. Sci.*, v. 264, p. 698-794.
- Gilligan, T.E., 1948, The solubility and transfer of silica and other non volatiles in steam: *Econ. Geology*, v. 43, p. 241-271.
- Goldschmidt, V.M., 1922, On metasomatic processes in silicate rocks: *Econ. Geology*, v. 17, p. 105-123.

- Goodwin, A.M., 1964, Geochemical studies at Helen Iron Range: *Econ. Geology*, v. 59, p. 684-718.
- Grantham, R.M., and Soule J.H., 1947, Jones iron deposit, Socorro County, New Mexico, U.S. Bur. Mines, Report of Investigation 4010, 6 p.
- Greig, J.W., et al, 1935, Equilibrium relationship of  $\text{Fe}_3\text{O}_4$ ,  $\text{Fe}_2\text{O}_3$  and oxygen: *Am. Jour. Sci.*, v. 30, p. 239-316.
- Greenwood, H.J., 1962, Metamorphic reactions involving two volatile phases: *Carnegie Inst. Washington, Yearbook*, v. 61, p. 82-85.
- Hamilton, D.L., Burnham, C.W., and Osborn, E.F., 1964, The solubility of water and effects of oxygen fugacity and water content on crystallization in mafic magmas: *J. Petrology*, v. 5, p. 21-39.
- Hawley, J.E., and Robinson, S.C., 1948, The supposed oxidation of  $\text{Fe}_3\text{O}_4$  by  $\text{CO}_2$ : *Econ. Geology*, v. 43, p. 603-609.
- Hemley, J.J., 1959, Some mineralogical equilibria in the system  $\text{K}_2\text{O}-\text{Al}_2\text{O}_3-\text{SiO}_2-\text{H}_2\text{O}$ : *Am. Jour. Sci.*, v. 257, p.241-270.
- Holland, H.D., 1959, Some applications of thermochemical data to problems of ore deposits: *Econ. Geology*, v. 54, p. 184-233.
- Holser, W.T., 1947, Metasomatic processes: *Econ. Geology*, v. 42, p. 384-395.
- Holser, W.T., and Schneer, C.S., 1961, Hydrothermal magnetite: *Geol. Soc. America Bull.*, v. 72, p. 369-386.
- Hormann, P.K., and Morteani, G., 1969, Quartzdiorite-granite contacts in Cima d'Asta pluton (North Italy): *Contr. Mineral. and Petrology*, v. 22, p. 361-367.
- Kalinin, D.V., 1962, Formation of magnetite in contact metasomatic magnetite deposits: *Geochemistry*, no. 7, p.722-727.
- 
- \_\_\_\_\_ 1969, Mechanism and kinetics of hydrothermal silicate production: *Geokhimiya*, no. 10, p. 1210-1216.



- Kelley, V.C., 1949, Geology and economics of New Mexico iron-ore deposits: The Univ. of New Mex. Press, Albuquerque, p. 213-223.
- \_\_\_\_\_ 1952, Tectonics of the Rio Grande depression of Central New Mexico, Guidebook of the Rio Grande County, Central New Mexico: New Mex. Geol. Soc., p. 93-105.
- Kelley, V.C., and Thompson, T.B., 1954, Tectonics and geology of the Ruidoso-Carrizozo region, Central New Mexico, Guidebook of the Ruidoso County, New Mex. Geol. Soc., p. 110-121.
- Kenneddy, G.C., 1950, A portion of the system silica-water: Econ. Geology, v. 45, p. 629-653.
- Kerr, P.F., 1959, Optical mineralogy: New York, McGraw-Hill Book Co., 442 p.
- Kerrick, D.M., 1960, Contact metamorphism in some areas of the Sierra Nevada, California: Geol. Soc. America Bull., v. 81, p. 2913-2938.
- Korzhinskii, D.S., 1959, The advancing wave acidic components in ascending solutions and hydrothermal acid-base differentiation: Geoch. Cosmochim., Acta 17, p. 17-20.
- Krauskopf, K.B., 1957, The heavy metal content of magmatic vapor at 600°C: Econ. Geology, v. 52, p. 786-807.
- \_\_\_\_\_ 1964, The possible role of volatile metal compounds in ore genesis: Econ. Geology, v. 59, p. 29-45.
- \_\_\_\_\_ 1967, Introduction to geochemistry: New York, McGraw-Hill Book Co., 721 p.
- Kullerud, G., and Yoder, H.S., 1959, Pyrite stability relations in the Fe-S system: Econ. Geology, v. 54, p. 533-573.
- Lamey, C.A., 1961, Contact metasomatic iron deposits of California: Geol. Soc. America Bull., v. 72, p. 669-677.
- Lasky, S.G., 1931, The system iron oxides: CO<sub>2</sub>:CO, and iron oxides: H<sub>2</sub>O:H<sub>2</sub>, as applied to limestone contact deposits; Econ. Geology, v. 26, p. 485-495.

- Leake, B.E., Hendry, G.L., Kemp, A., Plant, A.G., Hasvey, P.K., Wilson, J.R., Coats, J.S., Aucott, J.W., Lunel, T., and Howarth, R.J.L., 1969-1970, The chemical analysis of powders by automatic X-ray fluorescence: *Chem. Geology*, no. 5, p. 7-86.
- Lindgren, W., Graton, L.C., and Gordon, C.H., 1910, The ore deposits of New Mexico: U.S. Geol. Survey, Prof. Paper 68, 361 p.
- Lindgren, W., 1925, Metasomatism: *Geol. Soc. America Bull.*, v. 36, p. 247-261.
- \_\_\_\_\_ 1933, Mineral deposits: New York, McGraw-Hill Book Co., Inc., 930 p.
- Lepp, H., 1957, Stages in oxidation of magnetite: *Am. Mineralogist*, v. 42, p. 679-681.
- Loomis, A.A., 1966, Contact metamorphic reactions and processes in the Mt. Tallac roof remnant, Sierra Nevada California: *J. Petrology*, v. 7, p. 221-245.
- Mackin, H.J., and Ingerson E., 1960, An hypothesis for the origin of ore forming fluid: U.S. Geol. Survey Research, B1-B2.
- Mackin, H.J., 1968, Iron ore deposits of the Iron Spring District Southwestern Utah, in *Ore Deposits of United States*: New York, Am. Inst. Mining. Metall. Engineers, v. 2.
- Martin, R.F., and Piwinskii, A.J., 1969, Experimental data bearing on the movement of iron in an aqueous vapor: *Econ. Geology*, v. 64, p. 798-803.
- Merrin, S., 1960, Synthesis of epidote and its apparent P-T stability curve: *Geol. Soc. America Bull.*, v. 71, p. 1929.
- Morey, G.W., and Hesselgesser, I.M., 1951, The solubility of some minerals in superheated steam at high pressures: *Econ. Geology*, v. 46, p. 821-835.
- Morey, G.W., 1957, The solubility of solids in gases: *Econ. Geology*, v. 52, p. 225-251.

- Mueller, R.F., 1960, Compositional Characteristics and equilibrium relations in mineral assemblages of a metamorphosed iron formation: *Am. Jour. Sci.*, v. 258, p. 449-497.
- Newman, A., 1948, On hydrothermal differentiation: *Econ. Geology*, v. 43, p. 77-83.
- Nockolds, S.R., 1954, The average composition of the major igneous rock types: *Geol. Soc. America Bull.*, v. 65, p. 1007-1032.
- Osborne, F.F., 1928, Certain titaniferous magnetite deposits and their origin: *Econ. Geology*, v. 23, p. 724-761.
- Osborn, E.F., 1959, Role of oxygen pressure in the crystallization and differentiation of a basaltic magma: *Am. Jour. Sci.*, v. 257, p. 609-647.
- Ovchinnikov, L.N., 1960, Some regular phenomena in the magnetogene ore genesis: *Internat. Geol. Cong.*, 21st., Norden 1960, p. 7-17.
- Park, Ch.F., and McDiarmid, R.A., 1970, *Ore deposits: San Francisco, W.H. Freeman and Co.*, 522 p.
- Perry, D.V., 1969, Skarn genesis at Christmas mine, Gila County Arizona: *Econ. Geology*, v. 64, p. 255-270.
- Poldervaart, A., and Parker, A.B., 1964, The crystallization index as a parameter of igneous differentiation in binary variation diagrams: *Am. Jour. Sci.*, v. 262, p. 281-289.
- Ramberg, H., 1952, *The origin of metamorphic and metasomatic rocks: The University of Chicago Press*, 315 p.
- Ridge, J.D., 1949, Replacement and the equating of volume and weight: *Jour. Geology*, v. 57, p. 522-550.
- Robie, R.A., and Waldbaum, D.R., 1968, Thermodynamic properties of minerals and related substances at 298.15°K (25.0°C) and one atmosphere (1.013 bars) pressure and at higher temperatures: *U.S. Geol. Survey, Bull.* 1259, 256 p.

- Roy, D.M., and Rustum, R., 1955, Synthesis and stability of minerals in the system  $MgO-Al_2O_3-SiO_2-H_2O$ : Am. Mineralogist v. 40, p. 147-178.
- Ruiz, F.C., Moraga, A., and Aguilar, A., 1968, Genesis of the Chilean iron ore deposits of Mesozoic age: Internat. Geol. Cong., 23rd., Prague 1968, v. 7, p. 323-338.
- Sales, R.H., 1962, Hydrothermal versus syngenetic theories of deposition: Econ. Geology, v. 57, p. 721-734.
- Shand, S.J., 1944, The terminology of the late magmatic and postmagmatic processes: Jour. Geology, v. 52, p. 342-350.
- \_\_\_\_\_ 1947, The genesis of intrusive magnetite and related ores: Econ. Geology, v. 48, p. 14-38.
- \_\_\_\_\_ 1947, Eruptive rocks: New York, John Wiley and Sons, 488 p.
- Smith, F.G., 1948, Transport and deposition of non-sulphide vein minerals III. Phase relation at the pegmatitic state: Econ. Geology, v. 43, p. 553-546.
- \_\_\_\_\_ 1949, Laboratory testing of pneumatolitic deposits: Econ. Geology, v. 44, p. 624-625.
- \_\_\_\_\_ 1953, Review of physico-chemical data on the state of supercritical fluids: Econ. Geology, v. 48, p. 14-38.
- \_\_\_\_\_ 1963, Physical geochemistry: Massachusetts, Addison-Wesley Publ. Co. Inc., 624 p.
- Smith, J.R., and Yoder H.S., 1955, Variations in X-ray powder diffraction patterns of plagioclase feldspar: Am. Mineralogist, v. 41, p. 632-647.
- Stringham, B., 1952, Fields of formation of some common hydrothermal alteration minerals: Econ. Geology, v. 47, p. 661-664.
- Travis, R.B., 1955, Classification of rocks: Colorado School of Mines Quart., v. 50, p. 1-98.

- Thompson, J.B., 1959, Local equilibrium in metasomatic processes, in *Researches in Geochemistry*: New York, John Wiley and Sons, Inc., 511 p.
- Wahlstrom, E., 1950, *Introduction to theoretical igneous petrology*: New York, John Wiley and Sons, Inc., 365 p.
- Wells, F.G., 1938, The origin of the iron ore deposits in the Bull Valley and Iron Spring Districts, Utah: *Econ. Geology*, v. 33, p. 477-507.
- Wilpolt, R.H., and Wanek, A.A., 1952, *Geology of the region from Socorro and San Antonio East to Chupadera Mesa, Socorro County, New Mexico*: Geol. Survey Oil and Gas Inv. Map OM-21.
- Yoder, H.S., 1950, Stability relations of grossularite: *Jour. Geology*, v. 58, p. 221-253.
- Yoder, H.S., and Tilley, C.E., 1962, Origin of basalt magma: an experimental study of natural and synthetic rock systems: *Jour. Petrology*, v. 3, p. 342-532.

## Appendix I

Instrumental Parameters  
-x- ray fluorescence

|                      | Zn   | Rb      | Sr      | Fe     |
|----------------------|------|---------|---------|--------|
| Peak                 | K    | K       | K       | K      |
| Detector             | gfpc | scin    | scin    | gfpc   |
| Detector             | 1.05 | 1.10    | 1.08    | 1-1.20 |
| Detector<br>gas flow | P-10 | nat.gas | nat.gas | P-10   |
| Crystal              | Lif  | Lif     | Lif     | Lif    |
| Path                 | air  | air     | air     | air    |

Mo Tube

|                      | Mg          | Si   | S    | K    | Ca   | Ti   | Na          | Al   |
|----------------------|-------------|------|------|------|------|------|-------------|------|
| Peak                 | K           | K    | K    | K    | K    | K    | K           | K    |
| Detector             | gfpc        | gfpc | gfpc | gfpc | gfpc | gfpc | gfpc        | gfpc |
| Detector             | 2.64        | 1.70 | 1.69 | 1.66 | 1.66 | 1.64 | 2.48        | 1.70 |
| Detector<br>gas flow | nat.<br>gas | P-10 | P-10 | P-10 | P-10 | P-10 | nat.<br>gas | P-10 |
| Crystal              | gyp         | eddt | eddt | eddt | eddt | eddt | gyp         | eddt |
| Path                 | vac.        | vac. | vac. | vac. | vac. | vac. | vac.        | vac. |

Cr Tube

gfpc : gas flow propotional counter  
 scin : scintilation counter  
 vac : vacuum  
 Lif : Lithium fluoride

## APPENDIX II, part 1.

## Calibrations for Intermediate Igneous Rocks

$$\text{Na}_2\text{O}\% = 6.087 X - 4.858$$

$$\text{MgO}\% = 14.60 X + 0.167$$

$$\text{Al}_2\text{O}_3\% = 11.895 X - 0.492$$

$$\text{SiO}_2\% = 51.846 X - 6.968 X^2 - 1.208$$

$$\text{K}_2\text{O}\% = 0.921 X$$

$$\text{TiO}_2\% = 0.581 X$$

$$\text{CaO}\% = 9.112 X$$

$$\text{Fe}_2\text{O}_3\% = 10.340 X - 0.193$$

$$\text{Zn ppm} = 135 X$$

$$\text{Sr ppm} = 251 X$$

$$\text{S ppm} = 450 X$$

## APPENDIX II, part 2.

## Calibrations for Carbonate and Sulfate Rocks

|                           |   |  |
|---------------------------|---|--|
| $\text{Na}_2\text{O}\%$   | = | 6.895 X                                |
| $\text{MgO}\%$            | = | 16.785 X + 0.840                       |
| $\text{Al}_2\text{O}_3\%$ | = | 13.363 X + 0.836                       |
| $\text{SiO}_2\%$          | = | 30.236 X                               |
| $\text{K}_2\text{O}\%$    | = | 0.715 X - 0.014                        |
| $\text{TiO}_2\%$          | = | 1.021 X - 0.301 X <sup>2</sup> + 0.037 |
| $\text{CaO}\%$            | = | 6.980 X + 1.476                        |
| $\text{Fe}_2\text{O}_3\%$ | = | 10.50 X + 0.26                         |
| Zn ppm                    | = | 159 X                                  |
| Sr ppm                    | = | 275.5 X                                |
| S ppm                     | = | 337 X                                  |



APPENDIX III, part 1.

## Calibrations for Acid Igneous Rocks

$$\text{Na}_2\text{O}\% = 6.087 X - 4.858$$

$$\text{MgO}\% = 9.5 X$$

$$\text{Al}_2\text{O}_3\% = 14.156 X - 0.492$$

$$\text{SiO}_2\% = 57.549 X - 7.734 X^2 - 2.467$$

$$\text{K}_2\text{O}\% = 2.5 X + 0.20$$

$$\text{TiO}_2\% = 0.66 X$$

APPENDIX III, part 2.

## Calibrations for Basic Igneous Rocks

$$\text{Na}_2\text{O}\% = 6.067 X - 0.116$$

$$\text{MgO}\% = 15.50 X + 0.47$$

$$\text{Al}_2\text{O}_3\% = 9.232 X + 3.590$$

$$\text{SiO}_2\% = 51.846 X - 6.968 X^2 - 1.208$$

$$\text{K}_2\text{O}\% = 0.924 X - 0.061$$

$$\text{TiO}_2\% = 0.768 X - 0.206$$

$$\text{CaO}\% = 8.218 X + 0.151$$

$$\text{Fe}_2\text{O}_3\% = 12.294 X - 1.10$$

$$\text{Zn ppm} = 159 X$$

$$\text{Sr ppm} = 275.5 X$$

$$\text{S ppm} = 400 X$$

## APPENDIX IV.

## 1) Calculation of tonnage of iron leached from border facies

Length of the dike = 3000 m.

Width of the border facies = 30 m.

Depth considered for calculation = 200 m.

Diorite density = 2.84.

Iron leached as  $\text{Fe}_2\text{O}_3$  = 2% (weight)

$3000 \times 30 \times 200 \times 2.84 \times 0.02 = 1,020,000$  metric tons of iron  
as  $\text{Fe}_2\text{O}_3$ .

2) Calculation of the maximum amount of iron that could be transported by lateral sweating of deuteritic fluids from the dike.

Length of the dike = 3000 m.

Width of the dike = 200 m.

Depth considered for calculation = 200 m.

Diorite density = 2.84.

Iron transported by aqueous fluid = 1000 ppm.

Water in the dike = 8% (weight)

$3000 \times 200 \times 200 \times 2.84 \times 0.08 \times 0.001 = 27,200$  metric tons  
of Fe.

$\frac{27,200 \times 159.70}{111.70} = 38,888$  metric tons of  $\text{Fe}_2\text{O}_3$

This thesis is accepted on behalf of the faculty of the  
Institute by the following committee:

John E. Cooper

Clay T. Smith

Max E. Willard

\_\_\_\_\_  
\_\_\_\_\_

Date July 13, 1971